Regulation of Prostate Cancer Prostasomes by Polymerase I and Transcript Release Factor (PTRF)

Honours Thesis

24th October 2012

Jayde Ruelcke

Supervisor: Michelle Hill
Co Supervisor: Antje Blumenthal

Statement of Authorship

I, Jayde Ruelcke confirm that the work presented in this research proposal/research report has been performed and interpreted solely by myself except where explicitly identified to the contrary*. I confirm that this work is submitted in partial fulfilment for the degree of BSc Hons in Biomedical Science and has not been submitted elsewhere in any other form for the fulfilment of any other degree or qualification.

Word Count (excluding reference list, fig. Legends, tables and appendices): 7962 words

Dated: 24/10/2012

Signature: _____

* A student may often find that some work may be performed on their behalf. For example, histology preparations may be created by a member of the technical staff or surgery may be performed by another member of a laboratory. Such assistance must be accurately attributed and acknowledged.

I, Michelle Hill confirm that I have seen a copy of the work presented in this research proposal/research report as the supervisor of Jayde Ruelcke

Date: 24/10/2012

Signature: _____

Files and lab notebooks are stored at the University of Queensland Diamantina Institute.

Contents:

Included Figures:

Included Tables:

Included Diagrams

List of abbreviations

CHMP5	Charged Multivesicular Body Protein 5
CM	Conditioned Media
GFP	Green Fluorescent Protein
GRASP65	Golgi Reassembly-Stacking Protein 1
HPLC	High Performance Liquid Chromatography
IFN-γ	Interferon Gamma
IL-12, IL-23, IL-10, IL-1β, IL-6, IL-8	Interleukin - 12, 23, 10, 1-Beta, 6, 8
kcps	Kilo counts per second
LPS	Lipopolysaccharide
MIF	Macrophage Migration Inhibitory Factor
mRNA	Messenger Ribonucleic Acid
MVB	Multi Vesicular Body
PBS	Phosphate Buffered Saline
Pro	Prostasomes
PMA	Phorbol 12-Myristate 13-Acetate
ppm	Parts per million
PSA	Prostate Specific Antigen
PTRF	Polymerase I Transcript Release Factor
RT-qPCR or qPCR	Real Time Quantitative Polymerase Chain Reaction
SDS-PAGE	Sodium Dodecyl Sulfate - Polyacrylamide Gel Electrophoresis
SILAC	Stable isotope labelling with amino acids in cell culture
TAM	Tumour Associated Macrophage
TBST	Tris Buffered Saline - Tween 20
TNFα	Tumour Necrosis Factor Alpha
TGF-β	Transforming Growth Factor Beta
(-)	Prostasome depleted conditioned media

Abstract

Prostate cancer is a common condition affecting a large proportion of the elderly male population. Caveolin-1 is a gene associated with prostate cancer progression, with modulation of the cellular secretome as a potential mechanism. Proteins secreted in small vesicles (termed prostasome to reflect their prostatic origin) may establish local and distal microenviroments for tumour metastasis. Recent work from our group shows that the oncogenic caveolin-1 can be sequestered by expression of PTRF, a co-factor protein required for formation of stable caveolae.

The current study aimed to investigate the affect of PTRF expression on the prostasome secretion pathway. Dynamic light scattering was used to analyse the secretion and size of prostasomes and mass spectrometry identified differences in protein expression. The non-classically secreted cytokine MIF was used as a model protein to understand potential mechanisms of trafficking and packaging of prostasomes. Immune functionality of prostasomes was investigated by treating monocytes or macrophages with prostasomes or prostasome depleted conditioned media.

Results indicate that PTRF decreases both the number of prostasomes released, their size and the abundance of a subset of proteins. Differentially secreted proteins were enriched in pathways that attenuate inflammation and cytoskeletal remodelling. The inflammatory effect may occur independently of monocytes or macrophages that were not influenced by prostasomes.

Interestingly, modulation of MIF secretion by PTRF was independent of the classical golgi secretory pathway. Prostasome proteomics revealed the multivesicular body-mediator protein CHMP5 as one of the most significantly down-regulated proteins upon PTRF

expression. Further work will be required to confirm the involvement and role of CHMP5 and the multivesicular body secretion pathway in PTRF-mediated prostasome suppression. Identification of the pathway may provide novel therapeutic targets for caveolin-1-positive prostate cancers.

Acknowledgements

I wish to give a huge thank you to my supervisor Dr. Michelle Hill for allowing me to become a part of the lab. Honours would not have been as enjoyable without the support and help she has provided me with all year.

My co-supervisor Dr. Antje Blumenthal must not go unrecognised. Her insight into the immunology part of this project was invaluable.

Thanks must also go to the rest of the Hill lab. Thank you to Deb Black, Sunny Moon, Kerry Inder, April Choi, Alok Shah and Dorothy Loo. Your help in troubleshooting problems and answering my incessant questions is greatly appreciated.

Particular thanks go to Dorothy Loo who shared her mass spec expertise and trained me on the cherished machine.

The Simpson and Saunders groups also deserve to be acknowledged for their help. They too shared their knowledge and answered my questions when our side of the lab was particularly quiet.

I am also grateful for the help of Dr. Sandrine Roy for the microscopy work, Dr. Oscar Haigh and Jana McCaskill for the Zetasizer work and Lara Petelin who showed me the beloved technique of prostasome purification.

The University of Queensland, Diamantina Institute and the School of Biomedical Sciences must be formally recognised for accepting me into the honours program.

Above all, I wish to thank my family and friends for their support all year. I would not have accomplished this without you.

Introduction:

Role of Caveolin-1 and PTRF in Prostate Cancer

Prostate cancer is one of the most commonly diagnosed cancers in men, accounting for 6% of all cancers (Jemal *et al.*, 2011). Most prostate cancers are not lethal, however, due to the difficulty of identifying aggressive cancers, some patients are given unnecessary treatments (Basch *et al.*, 2012). If the option of treatment is not taken, patients risk the cancer becoming metastatic whereby it usually forms secondary tumours within the bone and lymph nodes (Cheng *et al.*, 2012; Li *et al.*, 2012). Therefore, there is an urgent need to identify which patients have advanced prostate cancer.

Prior studies have identified caveolin-1 as a potential biomarker for prostate cancer progression. Caveolin-1 expression is increased in around 30% of all prostate cancers and significantly associates with advanced disease (Corn and Thompson, 2010). Caveolin-1 is a cholesterol binding membrane protein that forms pits at the plasma membrane termed caveolae (Bastiani and Parton, 2010). Caveolae structures are stabilized by the co-factor protein Polymerase I And Transcript Release Factor (PTRF) (Hill *et al.*, 2008).

Caveolae are contained within membrane domains knowns as lipid rafts. The detergent resistant membrane regions play a role in signaling processes and intracellular protein transport (Simons and Ikonen, 1997). Clear distinctions between the effects of the caveolae or the lipid raft themselves has not been established (Inder *et al.*, 2012). PTRF may facilitate in distinguishing which functions are mediated by the caveolae. Loss of PTRF results in caveolin-1 expression lying on a flat plasma membrane without distinctive flask shaped caveolae invaginations (Refer to Diagram 1).

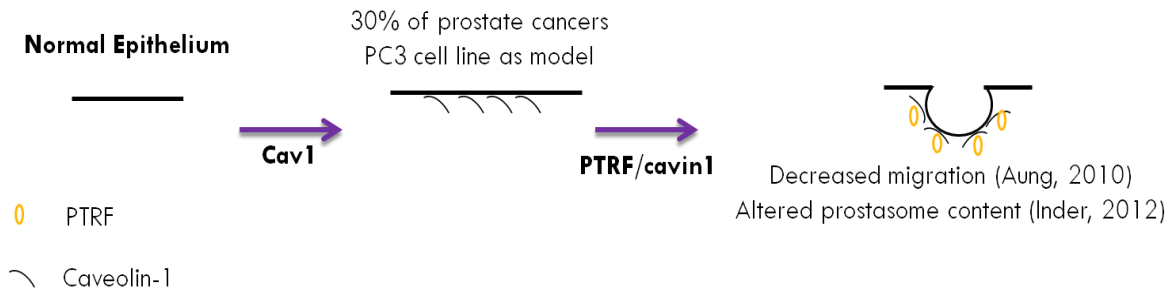

Diagram 1 The influence of PTRF and caveolin-1 on prostate cancer progression. In normal prostate epithelium, the plasma membrane lacks expression of both caveolin-1 and PTRF. Within prostate cancer up to 30% show caveolin-1 but not PTRF expression which localises to the flat plasma membrane. This can be modeled in the prostate cancer cell line PC3 that expresses caveolin-1 but not PTRF. Introduction of PTRF will enable formation of caveolae pits. Caveolin-1 forms oligomers for the basic pit structure which is stabilized by PTRF binding. This reduces the metastatic potential of the tumour and will have effects on secretion.

Recent published and unpublished work from our group show that caveolin-1 in prostate cancer is found in an aberrant form due to lack of expression of PTRF. The bone metastasis-derived PC3 cell line is a model of such aberrant caveolin-1 localization that also lacks endogenous PTRF expression (Hill *et al.*, 2008). By reintroducing the PTRF transcript into PC3 cells, caveolae formation is induced (Hill *et al.*, 2008), concomitant with reduced migratory ability and expression of matrix metalloproteinase 9 expression (Aung *et al.*, 2011). To determine the molecular mechanism, our laboratory performed subcellular proteomics analysis on these cell lines (Inder *et al.*, 2012). Protein changes were evident in total membrane and lipid raft fractions, as well as the total secretome and the vesicular secretome (termed prostasome) fractions (Inder *et al.*, 2012). PTRF expression reduced interleukin-6 (IL-6) secretion but not its total cellular levels, suggesting that PTRF specifically alters protein secretion (Inder *et al.*, 2012).

Interestingly, secreted IL-6 and TGF-β were identified in the prostasome fraction (Inder *et al.*, 2012). In view of the reported release of the membrane protein caveolin-1 from prostate cancer cells, down-regulation of prostasome-mediated cytokine release by PTRF could explain increased angiogenesis (Tahir *et al.*, 2009; Tahir *et al.*, 2001).

Secreted Microvesicles and Prostasomes

Recent studies demonstrate that secreted vesicles play a fundamental role in cancer progression. Released microvesicles are able to confer signals constitutive to cell proliferation (Hong *et al.*, 2009), survival, immune suppression (Abrahams *et al.*, 2003; Szczepanski *et al.*, 2011) and angiogenesis (Milsom *et al.*, 2007). While these can act locally through autocrine signalling (Al-Nedawi *et al.*, 2009a), they can be taken up by a range of cells both within the tumour and at distal sites where microvesicles can develop a niche

enabling preferential secondary tumour metastases to form (Grange *et al.*, 2011; Sidhu *et al.*, 2004).

Secreted vesicles are classified by their mode of secretion. Microvesicles generally denote vesicles that bud directly from the plasma membrane while exosomes are released from the multivesicular body (MVB) that forms by inward budding of endosomes (Duijvesz *et al.*, 2011) (Refer to Diagram 2). Vesicles released from the prostate gland, and prostate cancer cells have been termed prostasomes. Prostasomes are believed to follow the same release pathway as exosomes due to similarities in the morphological structure and lipid composition (Llorente *et al.*, 2007).

The prostasome and lipid raft components are highly related in structure, both being highly cholesterol rich (Arvidson *et al.*, 1989). Modulation of cellular cholesterol dynamics thus alters both fractions simultaneously in protein content (Llorente *et al.*, 2007). By changing the caveolae presence or distribution in cells, prostasomes too may be altered.

Previous studies performed in our lab indicate that prostasomes obtained from PC3 cells have a functional effect on osteoclastogenesis and osteoblast proliferation in vitro (unpublished), potentially mediating prostate cancer bone metastasis. Immune-suppression is another hallmark of cancer increasingly recognised as an essential component for tumour progression which may be mediated by tumour-secreted vesicles (Iero *et al.*, 2008). Identification of immune modulatory proteins (IL-6, MIF and TGF-β) within prostasomes further suggests a role for these vesicles in immune-modulation (Inder *et al.*, 2012).

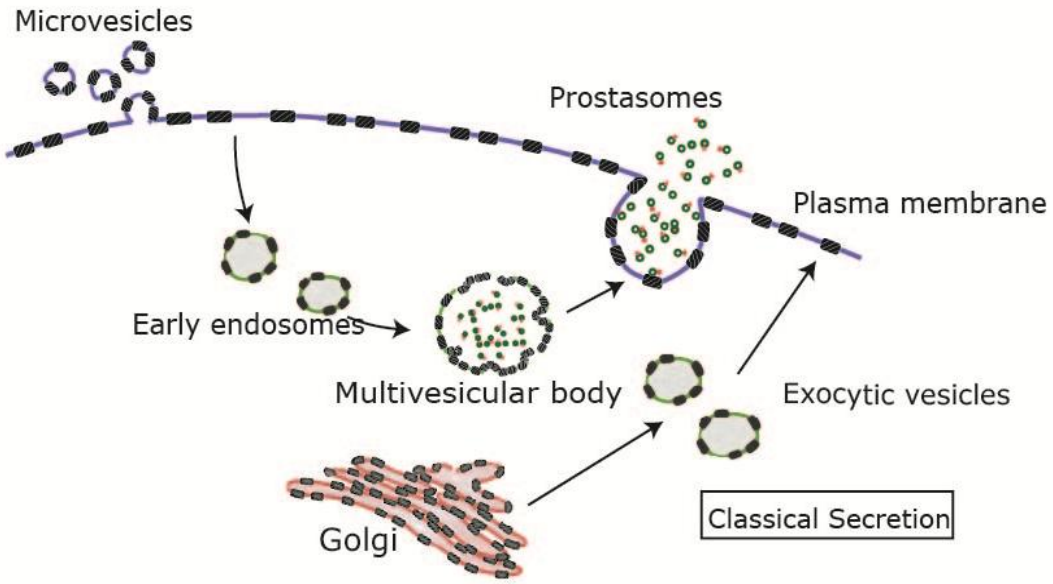

Diagram 2 Prostasomes are released in a non-classical secretion pathway. Prostasomes are derived from early endosomes that bud inwards to form a multivesicular body. Subsequent fusion with the plasma membrane will release the prostasomes into the surrounding cytosol.

Immune Modulation by Tumours

Immune modulation has previously been linked to prostate cancer aggressiveness and metastatic ability. This can occur through a range of alterations to the innate immune response (Davidsson *et al.*, 2012; Donkor *et al.*, 2011; Sotosek *et al.*, 2011). Macrophages are one particular target that show altered gene expression in a tumour microenvironment. This response is highly complex and requires a range of cytokines to be expressed to effectively alter differentiation pathways (Pello *et al.*, 2012). The response is also not homogenous and the tumour appears to polarise macrophages differently in the given microenvironment (Redente *et al.*, 2010).

Classically activated macrophages differentiate in response to IFN-γ either alone or in conjunction with bacterial stimuli such as LPS. When activated they are known as M1 macrophages and they have functional properties that elicit a TH1 and TH17 response. To polarise the TH1 and TH17 response they have high levels of IL-12, IL-23 and low IL-10 expression (Murray and Wynn, 2011). They also produce reactive oxygen and nitrogen intermediates for effective cell mediated killing and they can up-regulate the inflammatory cytokines IL-1β, TNFα and IL-6 (Mantovani *et al.*, 2005). Their overall response is to effectively kill cells and microorganisms whilst attracting other immune cells to the area and activate them (Mantovani *et al.*, 2002). Within a tumour, they exhibit anti-tumour functionality (Refer to Diagram 3).

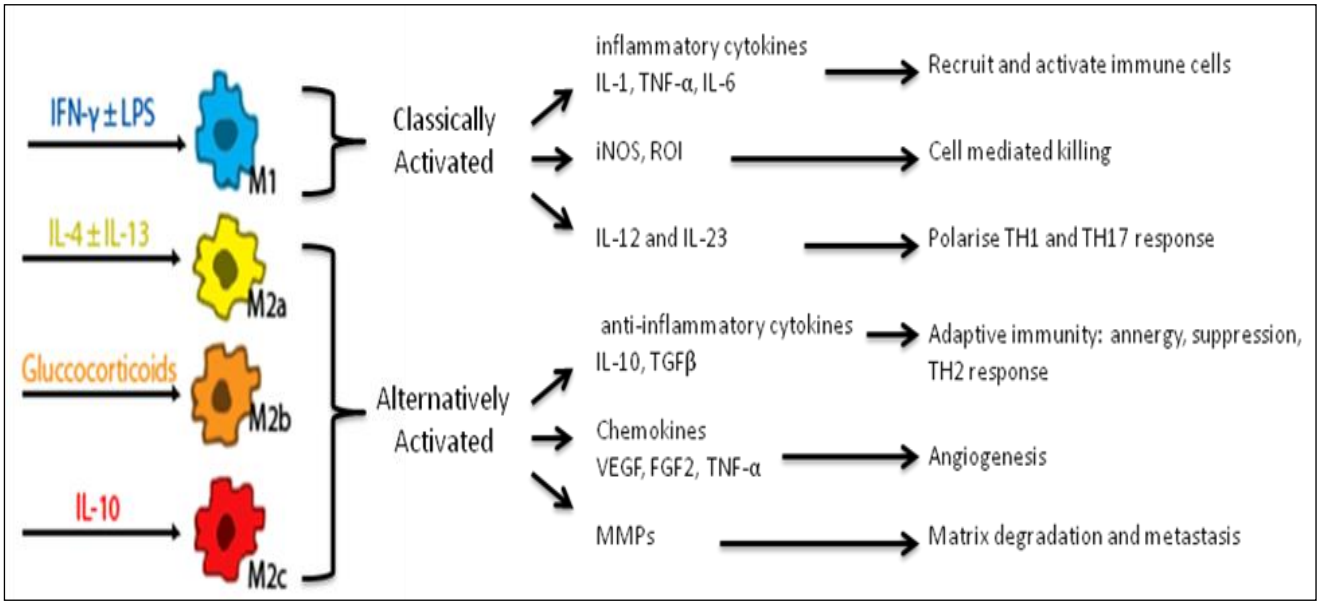

Diagram 3 Mechanisms of macrophage differentiation and their functional outcomes. Depending on the mode of activation, macrophages will have different tumour outcomes. Classically activated macrophages function to actively fight tumours while alternatively activated macrophages are associated with wound healing and repair, giving them characteristics that are in line with a pro-tumour response. This is dependent on the cytokines and molecules that they produce.

Within aggressive tumours, macrophages are typically found as M2 tumour associated macrophages (TAM). Biopsies taken from patients with malignant tumours show a higher degree of M2 markers in comparison with adjacent benign tissue (Redente *et al.*, 2010)**.** The presence of macrophages alone is sufficient to alter the aggressiveness of the tumour. Complete ablation of macrophages in mouse models can reduce metastatic ability and delay tumour progression (Lin *et al.*, 2001).

As an M2 phenotype, macrophages are able to further infiltrate a tumour and promote tumour survival (Scarpino *et al.*, 2000). They show low levels of IL-12 and IL-23 and high IL-10 (Murray and Wynn, 2011). Further differences arise depending upon their mode of activation and three pathways have been identified. IL-4 and IL-13, gluccocorticoids or IL-10 will polarise macrophages to M2a, b or c respectively. The exact differences between each of the M2 classes of macrophages has not been well characterised. It has been suggested that M2a show instances of wound healing through the release of growth factors and encouragement of angiogenesis (Gurtner *et al.*, 2008). M2c on the other hand enable immune suppression by encouraging a TH2 response that will up-regulate T-regulatory cells and myeloid derived suppressor cells (Mantovani *et al.*, 2004). Further models suggest that there are intermediates between the M2 classes of macrophages and some phenotypes may overlap (Mosser and Edwards, 2008). The presence of M2 macrophages within a tumour are consequently favourable for its growth. Their wound healing functionality can facilitate in metastasis, angiogenesis and immune suppression.

M2 macrophages are a specific subset of tumour associated macrophages. Depending on their state of polarisation they will express different receptors, perform different functions and produce different signalling molecules (Mantovani *et al.*, 2004). Their differentiation

profile is dependent on which molecules are present in the inflammatory microenvironment. Establishment of macrophage polarisation can then proceed down a classically or alternatively activated pathway (Mantovani *et al.*, 2004).

The immune modulatory effect of tumour secreted proteins has been demonstrated by taking conditioned media from tumour cells and adding it to monocyte macrophage precursors (Caras *et al.*, 2011). The resulting macrophages had differentiated down the path of the pro-tumour M2 phenotype. Due to the high plasticity of macrophages, existing M1 macrophages may also undergo transdifferentiation to an M2 phenotype (Biswas and Mantovani, 2010; Buhtoiarov *et al.*, 2011).

Hypothesis and aims

Based on the above, we hypothesized that PTRF expression down-regulates a population of oncogenic prostasomes which will have immune-suppressive function.

The aim of this study was to characterise the PTRF-down regulated population of prostasomes and to elucidate whether PC3 prostasomes can facilitate in establishing a new gene signature of macrophages, indicative of a pro-tumour phenotype. Specific aims are:

1. Determine the effect of PTRF expression on the size of prostasomes and cytokines released
2. Investigate the mechanism of cytokine release
3. Determine the effect of prostasomes on macrophage polarization

Methods

Reagents and Antibodies

The following reagents and antibodies were purchased from the following sources:

Tissue culture: Roswell Park Memorial Institute (RPMI) 1640 media and Trypsin-EDTA (Gibco), Fetal Bovine Serum (FBS) (HyClone), Phosphate Buffered Saline (PBS) (Amresco Inc), Geneticin G418 Selective Antibiotic (Invitrogen).

Antibodies:

Western blot - *Primary Antibodies*: Mouse anti-MIF (1/1000) (Sigma Aldrich), mouse anti-ERP57 (1/750) (Santa Cruz), rabbit anti-Cofilin (1/1000) and rabbit anti-EphA2 (1/1000) (Cell Signalling Technology). *Secondary Antibodies*: rabbit anti-Goat HRP, goat anti-mouse HRP, goat anti-rabbit HRP (all 1/3000) (Invitrogen).

Immunofluorescence - *Primary Antibodies*: Mouse anti-MIF (1/100) (Sigma), rabbit anti-GRASP65 (1/50) (BioLegend - Australia Biosearch). *Secondary Antibodies:* goat anti-mouse Alexa 647 (1/200), goat anti-mouse Alexa 568 (1/200), goat anti-rabbit Alexa 568 (1/200) (Invitrogen).

Cell Culture

PC3 cells stably expressing PTRF-GFP or GFP were previously reported (Aung *et al.* 2011). PTRF and caveolin-1 expression was confirmed by western blot prior to using the cells (data not shown). Cells were split at 80% confluency with 0.25% Trypsin-EDTA and used within seven passages. PC3 cells were maintained in RPMI1640 and supplemented with 5% FBS and Geneticin G418 selective antibiotics (0.1mg/mL).

THP1 cells were obtained from Antje Blumenthal. Cells were grown between $2x10^5$ and $2x10^6$ cells/mL in RPMI1640 supplemented with 10% FBS.

Prostasome Extraction

PC3 cells were grown to 80-90% confluency, whereby they were washed in PBS (phosphate buffered saline) and SFM (serum free media) was added. Conditioned media was collected after 24 hours. Media was spun at 800g for 5min followed by a spin at 5000g for 10min. Media was further concentrated in a 0.22µm Amicon Ultra-15 Centrifugal filter (Millipore). The remaining solution was spun at 100,000g for 2 hours before washing in PBS and repeating the spin. Prostasomes were resuspended in PBS and protein was quantified using a Bradford assay (Bio-Rad). Prostasomes were snap frozen and stored at -80^{o}C (Figure 1).

Western Blots

Whole cell lysates were collected by pelleting cells from a 15cm dish and treating with lysis buffer (1% Triton-X 100, 0.5mM sodium vanadate, 150nM NaCl, 20mM NaF, 05.mM 4-(2-Aminoethyl) benzenesulfonyl fluoride hydrochloride, 1µg /mL protease inhibitor cocktail, 20mM Tris pH 7.5). 10µg of prostasomes, prostasome depleted media or whole cell lysate was denatured by incubating for 5min at 95^{o}C with reducing SDS-PAGE sample buffer (2% SDS, 10% glycerol, 0.02% bromophenol blue, 50mM DTT, 40mM Tris pH 6.8). Samples were loaded onto a 10% SDS-PAGE gel. A wet transfer onto Polyvinylidene fluoride (PVDF) membrane (Millipore) was completed at 100V for 1 hour. Membranes were blocked in 5% skim milk powder and Tris-buffered saline with Tween-20 (TBST; 20mM Tris-HCl, 137 mM NaCl, 0.1% Tween-20, pH 7.5) for 30min and incubated with the primary antibody overnight at 4^{o}c. Membranes were washed in TBST and incubated at room temperature with the secondary HRP (horseradish peroxidase) antibody. Blots were developed on film (Fuji Super Rx medical x-ray film) using enhanced chemiluminescent (ECL) substrates (SuperSignal West Pico/Dura; Thermo Scientific).

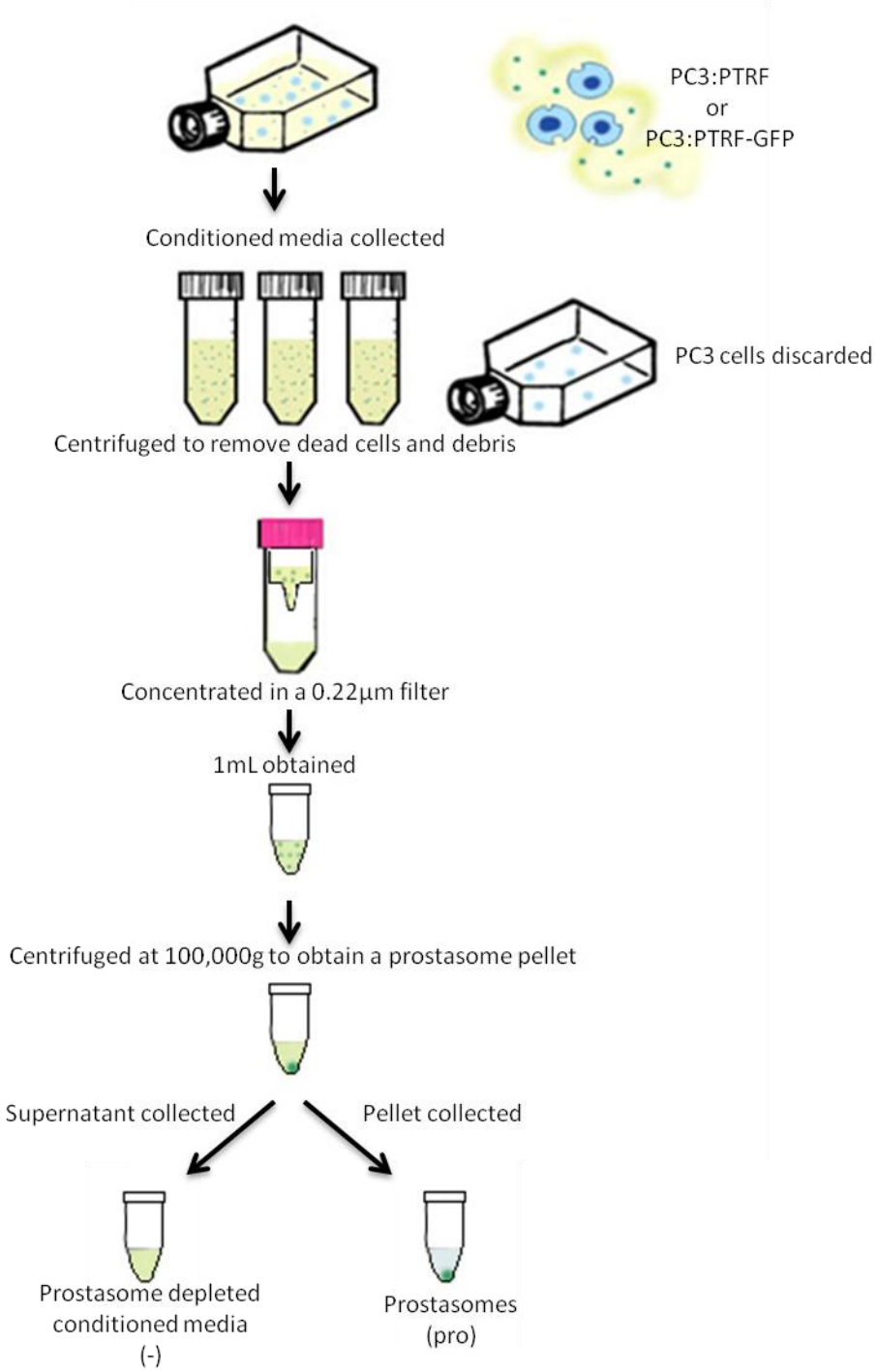

Figure 1 Schematic diagram of the prostasome extraction. Conditioned media is collected from PC3 cells before spinning to remove dead cells and cellular debris. The media is concentrated to 1mL using a 0.22um filter and is further spun at 100,000g to pellet the prostasomes. The supernatant is collected and used as prostasome depleted media while the prostasome pellet is washed in PBS before resuspension. (See methods for further detail).

Prostasome Size Analysis

Prostasome samples and prostasome depleted media were measured for size using the Zetasizer Nano ZS 90 (Malvern Instruments, Orsay, France). Each sample (30µg) was diluted in 1mL PBS and measured at 37°C in a glass cuvette with water as the dispersant. Size distribution and concentration were recorded as per the manufacturer's protocols. Concentration was normalised to the total cell number that collected prostasomes were derived from.

Proteomics

In-gel digest.

30µg of prostasomes were separated on a 10% SDS-PAGE gel to 8mm. The gel was stained with colloidal coomassie (20% methanol, 10% phosphoric acid, 10% ammonium sulfate, 0.12% CBB G-250) before destaining with 1% acetic acid. Protein loading was confirmed before excising each sample into 8x1mm pieces. Each gel band was destained with a solution of 50% acetonitrile:25 mM NH_4HCO_3. Samples were reduced with 20mM Dithiothreitol (DTT) followed by alkylation with 50mm Iodoacetamide (IAA). The samples were equilibrated to pH8 with 50 mM NH_4HCO_3 and subsequently dehydrated with 100% acetonitrile. Residual acetonitrile was removed with a SpeedyVac. Each gel piece was rehydrated with 0.2µg trypsin in 10% acetonitrile:50 mM NH_4HCO_3. The gel pieces were incubated with this trypsin solution at 37^{o}C overnight to allow digestion of proteins into peptides. Trypsin was deactivated with 5% formic acid. The peptides were extracted with 60% acetonitrile:1% formic acid and dried with a speedyvac. Peptides from each gel piece were resuspended in 10µl of 5% formic acid. Only 4µl of each peptide fraction was analysed by tandem mass spectrometry (Refer to figure 2).

LC-MS/MS.

A liquid chromatography-tandem mass spectrometer(LC-MS/MS) (Agilent 1200 HPLC and 6520 QTOF) coupled with a Chip CUBE was used to analyse the digested peptides. A HPLC (High Performance Liquid Chromatography) chip with 160nL C18 trapping column, and a 150mm C18 resolving column was used to separate the peptides (Agilent G4240-62010) using a combination of Buffer A (0.1% Formic acid) and Buffer B (0.1% Formic: 90% Acetonitrile) for sample analysis. A capillary HPLC was used to load the samples onto the HPLC trapping column at a flow rate of 4µl/min, 3% buffer B. A nano HPLC was used to elute the samples from the HPLC analysis column at a flow rate of 0.3µl/min, with a 5% to 50% gradient of buffer B over 45 min. Remaining peptides were cleared by washing with 95% Buffer B for 3mins. The column was equilibrated with 5% buffer B for 10mins.

The mass spectrometer enabled detection of 8 MS1 spectra/second and 4 MS/MS spectra per second. Peptides were excluded from MS/MS analysis for 15 seconds if 2 identical spectra were obtained consecutively.

Database searching.

LC-MS/MS raw data was processed with Agilent's Spectrum Mill. Selected modifications included fixed carbamidomethylation of cysteine and variable oxidation of methionine. Results were searched with the SwissProt database against Homo Sapiens. Trypsin was selected for enzyme digest, with 2 maximum missed cleavages allowed. The precursor mass tolerance was set at +/- 20ppm and product mass tolerance was +/- 50ppm. Only proteins with peptide score >10, protein score >11, scored peak intensity > 60% were selected. Results were validated with a false discovery rate of 0.5%.

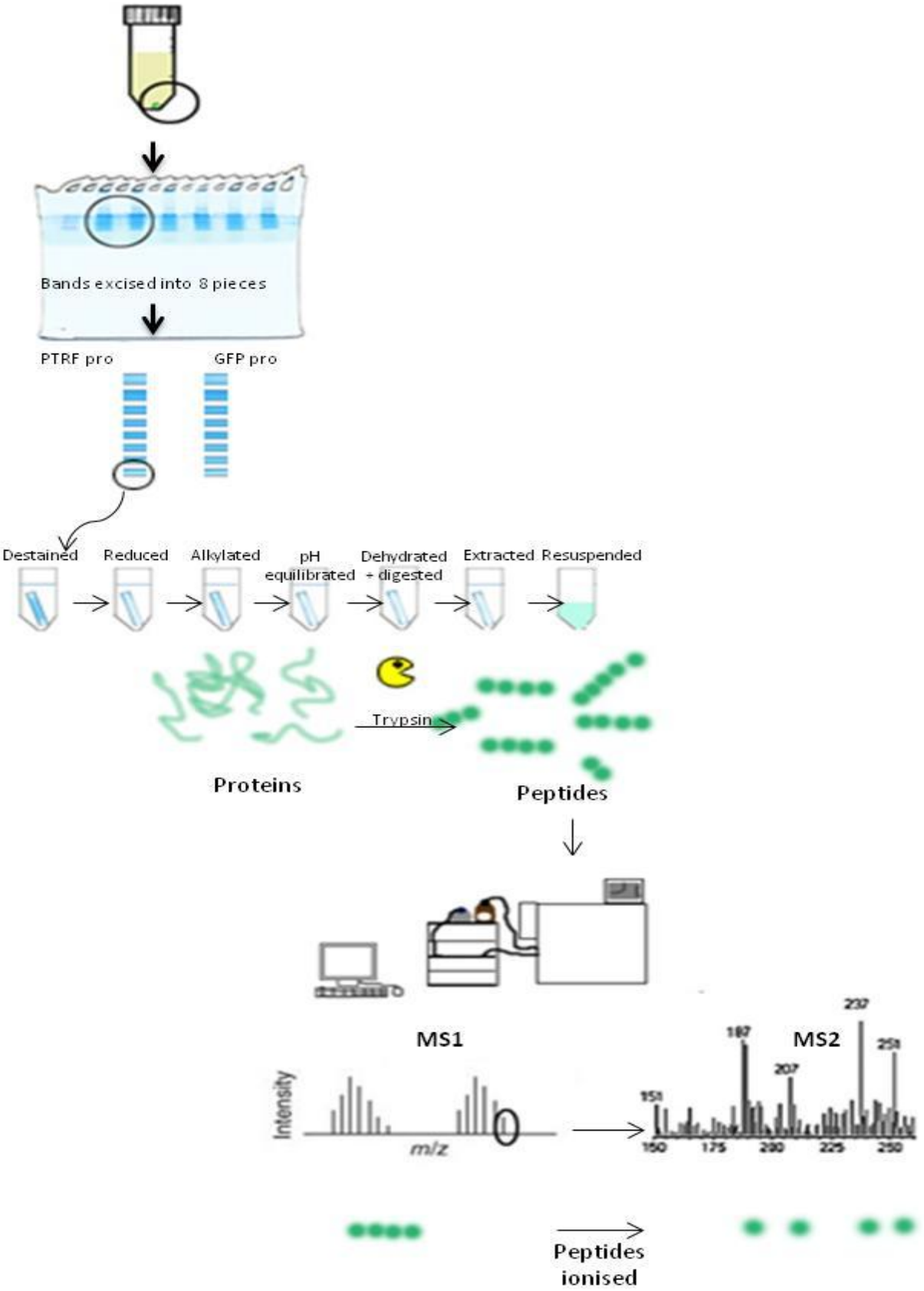

Figure 2 Schematic representation of the mass spectrometry protocol. Prostasomes were run on an SDS-PAGE gel and cut into eight pieces. Each fragment was destained and digested with trypsin. The small peptides were loaded onto a HPLC chip and eluted. MS1 of the peptide fragments was determined before ionisation and determination of the peptide sequence based on the MS2 spectra.

Pathway analysis

Normalisation was performed by comparing individual protein intensities or spectral counts to the total intensity or count for each individual sample. The resulting proportion was statistically analysed. Genego Metacore pathway analysis was used to analyse proteomic results. All identified proteins were used as a background list while those significantly different were used to generate process and pathway networks. The false discovery rate was set at 0.05.

BFA treatment

Cells were treated with 0.1ug/mL Brefeldin A (BFA) (Sigma Alrich) for 20 hours before fixing.

Immunofluorescence

PC3 cells were grown on coverslips. Experiments utilising Lyso-Tracker, ER-Tracker or Mito-Tracker (Invitrogen) were used as per manufacturers protocols. Cells were fixed in 4% paraformaldehyde for 30min before permeabilising in 0.1% triton X and 5% BSA in PBS for 30min. They were further incubated with the primary and secondary antibodies for 1hr each. Coverslips were mounted in ProLong Gold (Invitrogen) before imaging on the Ziess 510 Meta Confocal Microscope. Images were acquired with Zen 2009 software and compiled in Adobe Photoshop CS5.

THP1 differentiation

$1x10^6$ THP1 cells were grown in 6 well plates in SFM. Cells were treated with 5µM PMA (Phorbol 12-myristate 13-acetate) and either 25ng/mL of IFN-γ and 1mg/mL LPS, 25ng/mL IL-4 and IL-13 or 25ng/mL IL-10 for M1, M2a and M2c controls respectively. For transdifferentiation experiments, THP1 cells were first differentiated for 48 hours with the

addition of 25ng/mL of IFN-γ and 1mg/mL LPS. 30µg of prostasomes (resuspended in PBS) or prostasome depleted media were used for the treatment groups. Media was removed after 72 hours for differentiation experiments or 48hours for transdifferentiation experiments. Adherent cells were treated with Trizol. All cells were collected for THP1 and treatment groups by centrifuging media for 5 minutes before both the cell pellet and adherent cells were treated with trizol (refer to figure 3).

qPCR

RNA was extracted from THP1 cells following treatment with Trizol (Invitrogen). Isolated RNA was quantified and checked for integrity using a NanoDrop ND1000 (Thermo Fisher) before treating 2µg of RNA with DNAse I (Ambion). cDNA was created using a Tetro cDNA synthesis kit (BioLine). qPCR was performed with SYBR Premix Ex Taq (Tli RNaseH Plus) (Takara) on an AB7900 thermal cycler (Agilent). Cycling conditions consisted of an initial denaturation at 95^{o}c for 1 minute followed by 40 cycles of 95^{o}c for 15 seconds and 60^{o}c for 30 seconds. The dissociation stage consisted of 15 seconds at 95^{o}c followed by 90 seconds at 60^{o}c and 15 seconds at 95^{o}c. No Reverse Transcriptase controls were implemented for primers amplifying a product within the same exon. Primers are listed in table 1.

Statistical analysis

Results were analysed with GraphPad Prism 5. P values were obtained using a two-way unpaired Student's t-test or a paired repeated measures one-way Anova with a Tukey correction.

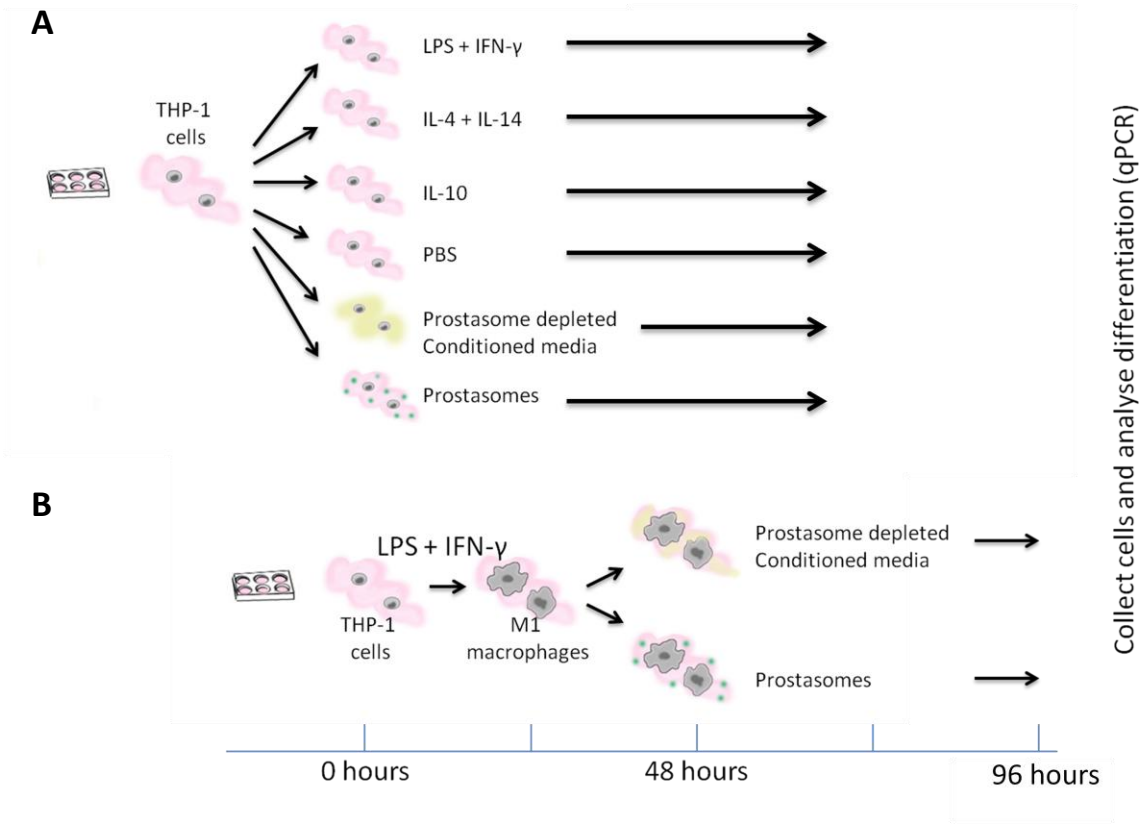

Figure 3 Schematic diagram of THP1 differentiation protocols. (A) In the differentiation protocol, THP1 monocytes were treated with LPS and IFN-γ, IL-4 and IL-13 or IL-10 as positive controls of macrophage differentiation. Alternately, cells either had no treatment or the addition of prostasomes or prostasome depleted media. mRNA was collected for analysis. (B) To analyse trandifferentiation, cells were first differentiated using LPS and IFN-γ before the addition of treatment groups. mRNA was collected to identify changes in relation to untreated cells.

Table 1 Primer sequences of genes analysed by qPCR

Gene Name	Forward Primer (5'-3')	Reverse Primer (5'-3')
TNF-α	CCCCAGGGACCTCTCTCTAA	CAGCTTGAGGGTTTGCTACA
TGF-β	AAGTGGACATCAACGGGTTC	TGCGGAAGTCAATGTACAGC
IL-1β	AGGCCGCGTCAGTTGTTGTG	GGAGCGTGCAGTTCAGTGATC
IL-12 p40	CCAGAGCATCTTTGACTGTG	CATTTGGTATCCATCCTTCACC
IL-6	AATTCGGTACATCCTCGACGG	TTGGAAGGTTCAGGTTGTTTTCT
IL-23	GGGAGACTCAGCAGATTCCAAGCC	TGCTGCTCCATGGGCAAAGAC
CD14	CACAGGACTTGCACTTTCCAG	CAGGATTGTCAGACAGGTCTAGG
β-actin	ATTGCCGACAGGATGCAGAA	GCTGATCCACATCTGCTGGAA

Results

Prostasomes were adequately purified from PTRF expressing PC3 cells

Prostasomes were prepared using a protocol previously published that utilises ultracentrifugation (Inder *et al.*, 2012), and the purity of the obtained prostasomes were confirmed by western blotting (Figure 4). Isolated prostasomes showed enrichment of the exosomal marker cofilin and was free from endoplasmic reticulum contaminants such as ERP57, hence the purity was deemed sufficient for experimentation (Mathivanan and Simpson, 2009).

PTRF affects the size distribution and concentration of secreted prostasomes

Previous studies from our lab used electron microscopy to examine the size of prostasomes (unpublished). The vesicles identified appeared to be of variable size between 100-150nm in diameter. To further investigate and quantitate the size of prostasomes, particle size was measured based on dynamic light scattering using the *Malvern Zetasizer Nano ZS*. Samples are illuminated with a laser and fluctuations in deflected light intensity due to brownian motion are measured and correlated to size. Equal prostasome protein or prostasome depleted conditioned media was diluted in PBS. Size analysis of the purified samples indicated that the prostasome fraction contained vesicles larger than 40nm. The majority of particles detected in the prostasome free fraction were smaller than 40nm. Prostasome free conditioned media contained no particles larger than 95nm (Figure 5A). This indicates prostasome purification protocols adequately separate conditioned media into two populations of samples.

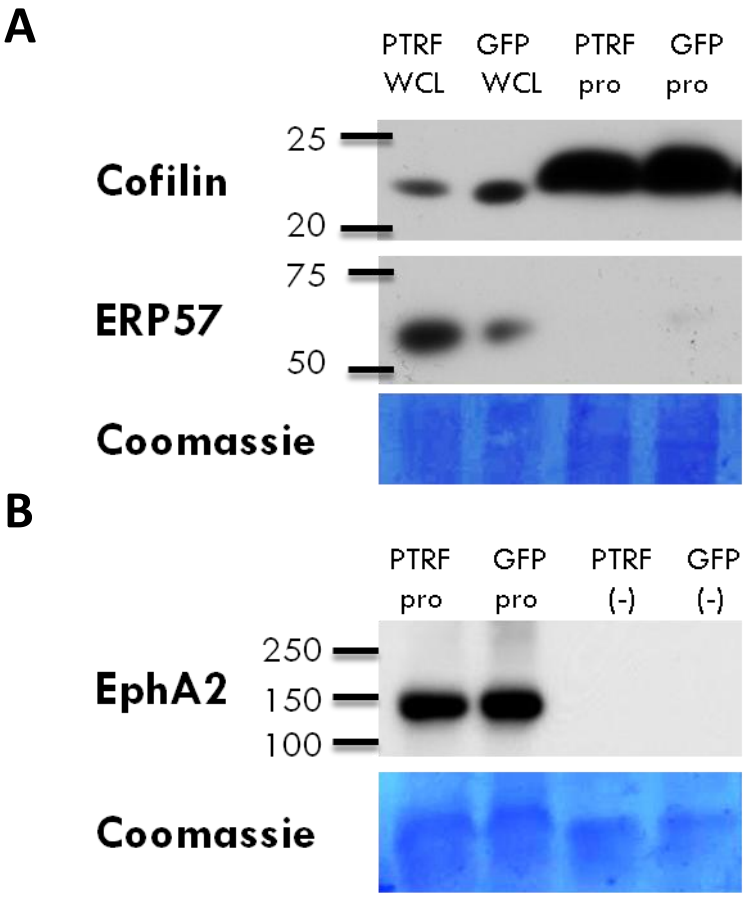

Figure 4 Prostasomes derived from PC3 cells were enriched in exosomal markers and were free from contaminants. (A) Cofilin but not ERP57 was enriched in both PTRF and GFP prostasomes in comparison to wole cell lysates (WCL). (B) Prostasome (pro) and prostasome depleted conditioned media (-) was free from exosomal contaminants. Blots are representative of 3 experiments. *GFP = PC3:GFP, PTRF = PC3:PTRF-GFP, WCL = Whole cell lysate, pro = prostasomes, (-) = prostasome depleted conditioned media.*

Of the vesicles greater than 40nm, particles extracted were the expected size for exosomes and/or microvesicles. Introduction of the PTRF transcript significantly reduced the size of particles released: Prostasomes secreted from PC3:PTRF-GFP cells were 156.4 ± 1.296nm making them smaller in size in comparison to PC3-GFP cells which were 178.8 ± 3.192nm (Figure 5B, p=0.0029).

When obtaining prostasomes, the purification protocol consistently resulted in a greater proportion of prostasomes being extracted from GFP cells. This was measured as a result of total prostasome protein. While this may be a result of larger particles carrying more protein, the cells may secrete an increased number of prostaomes. Dynamic light scattering analysis indicated that the number of prostasomes secreted per cell was significantly different (p=0.0023). PC3-GFP cells had detection rates of 7.456 ± 0.02726 kcps while PC3:PTRF-GFP detected 4.616 ± 0.4101 kcps for the same number of cells (Figure 5C). PC3-GFP cells were able to produce a higher concentration of prostasomes in the same volume of media. Together, these results show that PTRF expression reduced the size and concentration of prostasomes released from PC3 cells.

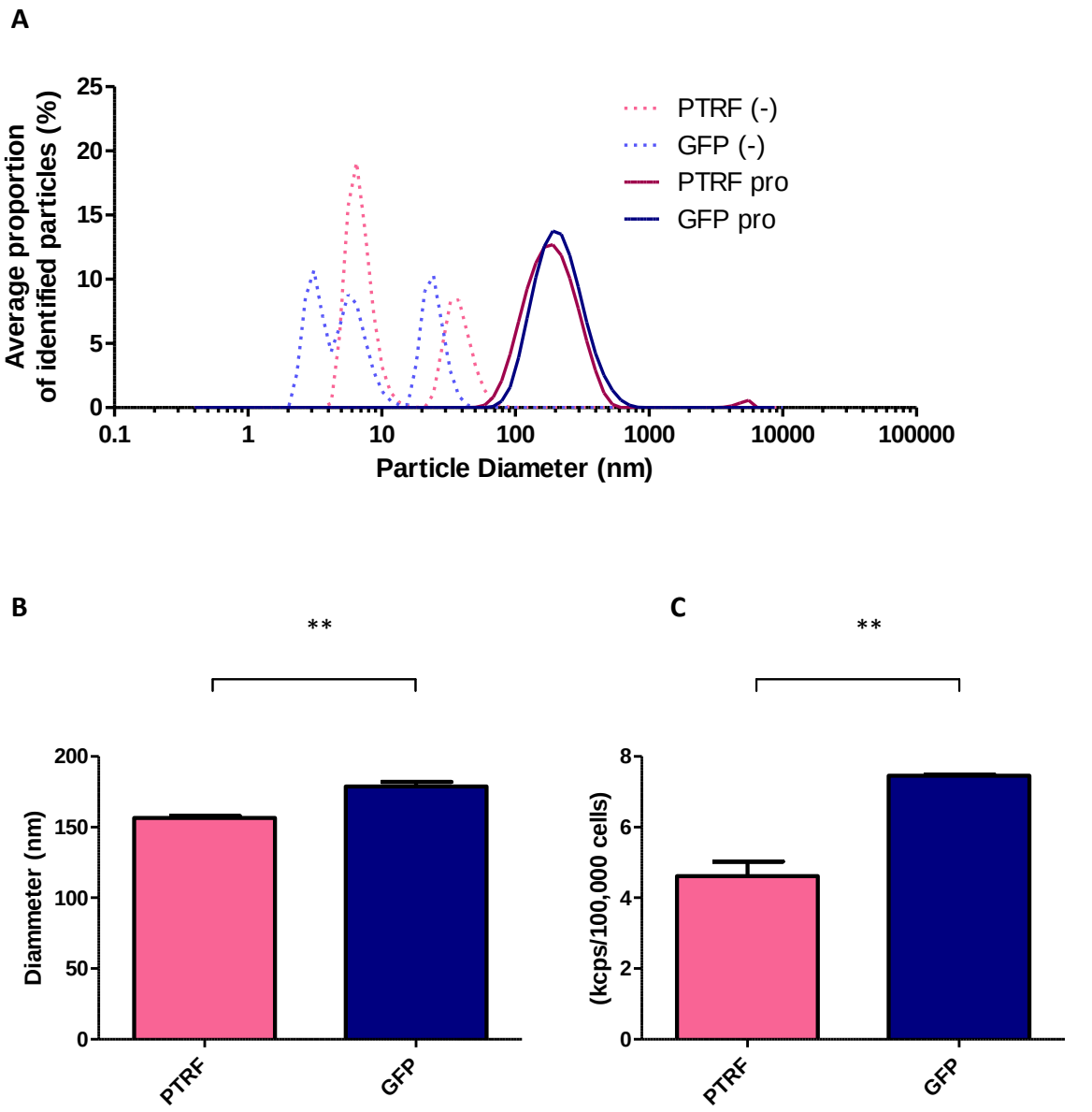

Figure 5 Prostasomes purified from cells expressing PTRF are decreased in both size and concentration. (A) Particles of prostasomes (solid lines) and prostasome-free conditioned media (broken lines) were examined using dynamic light scattering. (B) Mean particle diameter was significantly different for PTRF and GFP PC3 cells (p=0.0029 (C) The concentration of prostasomes secreted per cell was lower in cells transfected with PTRF (p=0.0023). *kcps = kilo counts per second.*

PTRF expression alters the protein composition of prostasomes

Proteins released via prostasomes can be transferred to target cells and exert function (Hao *et al.*, 2006). Previously our group carried out a quantitative SILAC (Stable isotope labelling with amino acids in cell culture) proteomics study that identified 367 proteins in the 2 cell lines (Inder *et al.*, 2012). SILAC can overcome issues of mass spectrometry sample bias by enabling samples to be run simultaneously (Ong et al., 2002; Zhang et al., 2011). By culturing cells with amino acids of different molecular weights, proteins will incorporate the different amino acids and peptides can be assigned to one of two samples (Ong *et al.*, 2002). SILAC is advantageous in that prostasome purification can be streamlined by combining samples at an earlier point. The previous study (Inder *et al.* 2012) combined conditioned media with equal total secretome protein. As our new results indicate that PC3:GFP cells release more prostasomes, this could lead to a higher proportion of PC3:GFP proteins being identified in the SILAC study, hence we performed an independent label-free quantitative proteomics study.

Equal amount (30µg) of prostasome proteins isolated from PTRF and GFP PC3 cells were separated by SDS-PAGE to 8 fractions. After in-gel tryptic digest, the peptides were analysed by LC-MS/MS.

We looked at the total list of proteins identified in both samples combined to identify whether results were consistent with other reports. A SILAC in-solution-digest protocol identified 367 prostasome proteins (Inder *et al.*, 2012), the current procedure identified 1082 proteins. Of these, 258 were found in both data sets (Figure 6A).

A

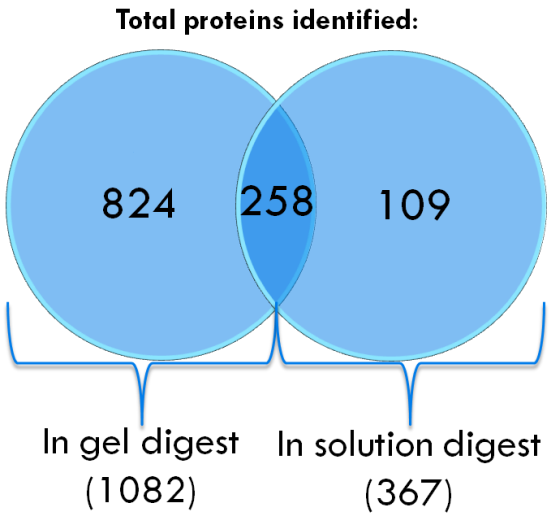

B

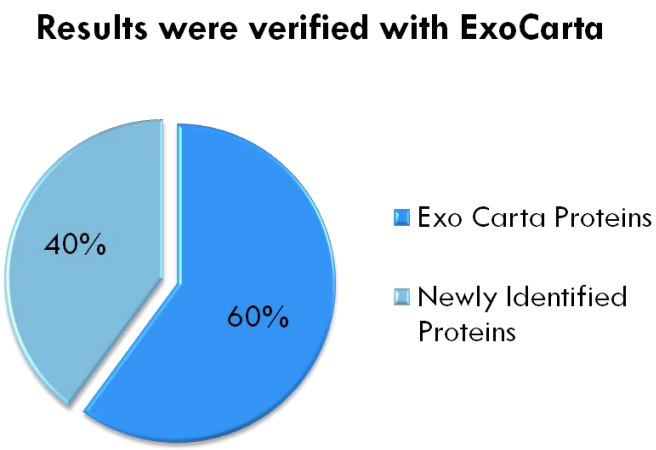

Figure 6. Comparison of prostasome proteomics data with previous studies. (A) Venn diagram showing overlap of identified proteins between a study utilising 'In solution digest' (Inder *et al.* 2012) and the current study. (B) Pie chart showing the proportion of proteins in the current study that were found in the *ExoCarta* database.

To ensure these were appropriate proteins for the prostasome/vesicle fraction, the total list was compared to Exocarta, an online database of all exosomal proteins (Mathivanan and Simpson, 2009). Only 60.13% of the identified proteins have been previously found within exosomes (Figure 6B) possibly due to limited data on prostate cancer exosomes (prostasomes). The database indicates 220 proteins have been previously identified in prostate cancer exosomes. This only takes into account one study that utilised different prostate cancer cell lines including androgen receptor negative (DU145 and PC3), androgen receptor positive (VCaP, LNCaP, and C4–2) and the benign epithelial prostate cell line RWPE-1 (Hosseini-Beheshti *et al.*, 2012). While 139 significant proteins were identified, only 27 overlapping proteins were found in PC3/DU145 cells compared to the other cell types (Hosseini-Beheshti *et al.*, 2012).

The number of proteins identified in our analysis, however, may indicate that we have a greater degree of detection that may have been missed in their study. Specific proteins previously identified only in the benign cell line RPWE1 (Hosseini-Beheshti *et al.*, 2012) were found in the both the PC3:PTRF and PC3:PTRF-GFP prostasomes. These include proteins such as Laminin gamma subunit 2. Others such as Thrombospondin, while found in the less aggressive C4-2 cells, as well as the benign, were also identified in our prostasomes. The levels of these were not significantly altered by PTRF expression

To identify proteins that were differentially expressed we performed label-free normalisation. For label-free quantitation, spectral intensity for each protein was normalized to the total spectral intensity for the biological sample. Similar analysis was completed based on the spectral count of each protein. Spectral count for each protein was normalized to the total number of spectra identified for each sample (Griffin *et al.*, 2010). While we wanted to

normalise to both spectral count and intensity simultaneously, we did not have access to the required software so normalisation was completed independently. Student's t-test was used with normalised data to determine the significant changes in protein expression across the 4 replicates.

Spectral intensity normalised results were used for comparison with the SILAC study (Inder *et al.*, 2012). To determine whether protein expression was consistent in the data sets, we analysed down regulated proteins. An average of the spectral intensity was identifed for the four independent samples in each treatment group. Down regulation was identified if the average absolute spectral intensity was lower for PTRF prostasomes in comparison to GFP. 100 proteins showed an overlap in downregulation of prostasome proteins (figure 7A).

Further or alternate normalisation methods may be used to validate the significantly altered proteins. It is suggested that some forms of normalisation do not reduce all replicate variability. Factors such as protein length can contribute to an increased detection rate (Ishihama *et al.*, 2005). Normalising for peptide length alone does not provide a better form of normalisation (Griffin *et al.*, 2010). Normalisation protocols must therefore be optimised and include a range of factors to avoid missing biologically significant results (Cairns *et al.*, 2008).

A

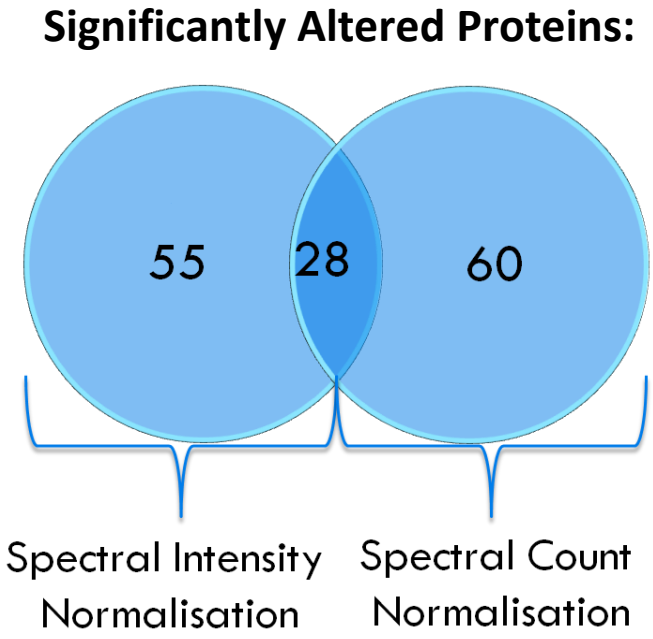

B

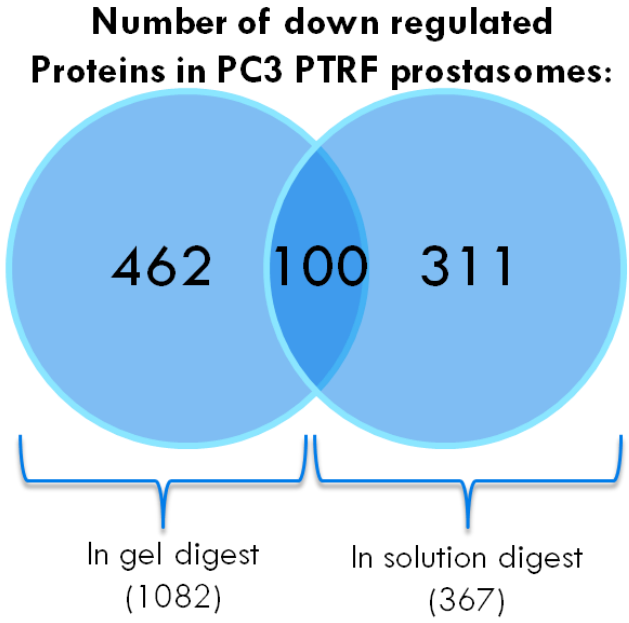

Figure 7 PTRF alters protein secretion in prostasomes. Venn diagrams showing the overlap of (A) proteins identified as being down-regulated in PTRF prostasomes on the basis of absolute average spectral intensity for our 'in gel digest' in comparison to an 'in solution digest' (Inder *et al.*, 2012). (B). Normalised prostasome proteins identified as significantly different following PTRF expression.

It has been reported that normalising for length in conjunction with both spectral count and spectral intensity can reduce sample inconsistencies (Griffin *et al.*, 2010). Normalisation of our data suggests that looking at the spectral count or spectral intensity alone resulted in different proteins being identified as significantly different. While there were a similar amount of proteins identified as significantly different ($p<0.05$), 55 for spectral intensity and 60 for spectral count, the proteins were not identical. Of those identified, only 28 were present in both lists (Figure 7B).

In future, these results will be verified in conjunction with peptide length based on the SI_N (Spectral Index) normalisation protocol or the subsequently derived normalized spectral abundance factor (NSAF) (Griffin *et al.*, 2010; Trudgian *et al.*, 2011; Trudgian *et al.*, 2010). This software was not available during data analysis of this study.

Only proteins identified through both normalisation methods were further investigated (Table 2). Investigation of the identified proteins list suggested that proteins associated with lipid rafts, the cytoskeleton and trafficking were differentially expressed. PTRF expression has been linked with changes to the lipid rafts (Inder *et al.*, 2012). Changes to lipid rafts subsequently affect the prostasomes as they are highly related. The lipid-raft protein flotilin-1 was differentially altered suggesting changes to the lipid rafts (Donatello *et al.*, 2012). Proteins such as Moesin, Plastin-2 and Tubulin Gamma 1 Chain all correlate with cytoskeletal regulation (Auvinen *et al.*, 2012) (Burkard *et al.*, 2011; Janji *et al.*, 2006). This is consistent with previous results that identify cytoskeletal regulatory pathways are enriched in PC3 cells following PTRF expression (Inder *et al.*, 2012). One protein, Charged Multivesicular Body Protein 5 (CHMP5), associated with trafficking was also differentially expressed. CHMP5

Table 2 Significantly different proteins identified within prostasomes following PTRF expression normalised to both spectral intensity and count

UniProt Accession Number	Protein Name
P13798	Acylamino-acid-releasing enzyme
P12830	Cadherin-1
Q9NZZ3	Charged multivesicular body protein 5
O00299	Chloride intracellular channel protein 1
Q9NY35	Claudin domain-containing protein 1
O75131	Copine-3
Q12959	Disks large homolog 1
Q12805	EGF-containing fibulin-like extracellular matrix protein 1
P19957	Elafin
P43003	Excitatory amino acid transporter 1
Q8IWU5	Extracellular sulfatase Sulf-2
O75955	Flotillin-1
P07900	Heat shock protein HSP 90-alpha
P26038	Moesin
Q15758	Neutral amino acid transporter B(0)
P13796	Plastin-2
P02545	Prelamin-A/C
Q9NRW3	Probable DNA dC->dU-editing enzyme APOBEC-3C
Q13275	Semaphorin-3F
O95084	Serine protease 23
P30626	Sorcin
P00750	Tissue-type plasminogen activator
P23258	Tubulin gamma-1 chain
P22314	Ubiquitin-like modifier-activating enzyme 1
Q9NYU2	UDP-glucose:glycoprotein glucosyltransferase 1
Q16222	UDP-N-acetylhexosamine pyrophosphorylase
Q9H1C7	UPF0467 protein C5orf32
P12955	Xaa-Pro dipeptidase

plays a role in lysosome sorting (Martin-Serrano *et al.*, 2003). CHMP5 was identified only in prostasomes from PC3:GFP cells and was completely absent in PTRF expressing cells. Understanding how such proteins affect trafficking may give an idea of how proteins are selectively sorted and altered in cells expressing PTRF.

The significantly different proteins were also analysed for pathway enrichment utilising the *Genego* software. Significantly different proteins were compared to a background list of all prostasome proteins identified through our mass spectrometry analysis. This facilitates in identifying enriched processes only as a result of PTRF attenuating prostasome packaging. Comparing to a background of all proteins may result in generic prostasome pathways being found. Interestingly, *genego* identified lymphatic metastasis as a disease based on given biomarkers ($p=1.452x10^{-5}$) (Figure 8A). This was identified in addtion to several other cancers and pre-cancer conditions. For the same proteins, processes related to cellular adhesion, cytoskeletal remodeling as well as inflammatory pathways were also found to be enriched processes (Figure 8B).

A .

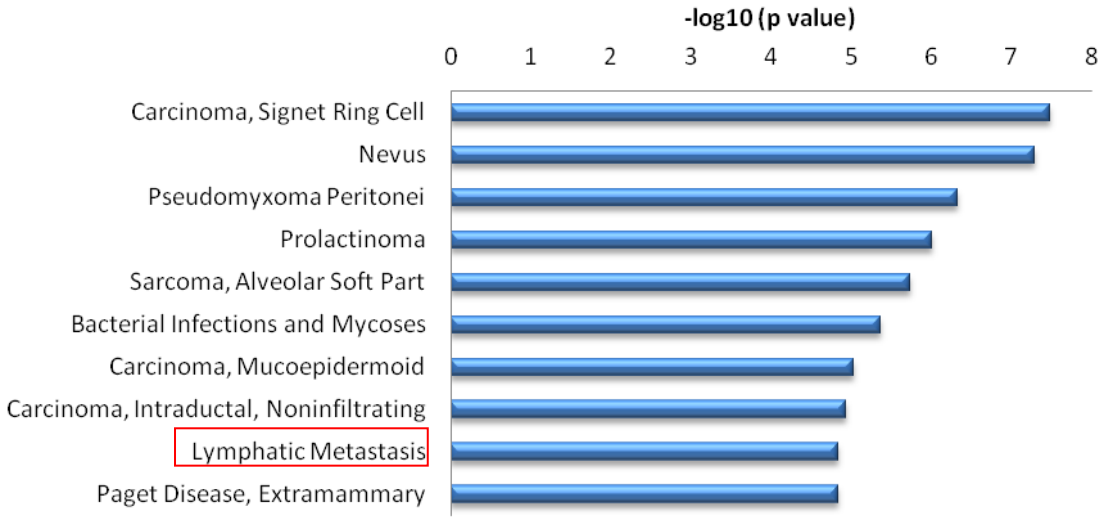

B

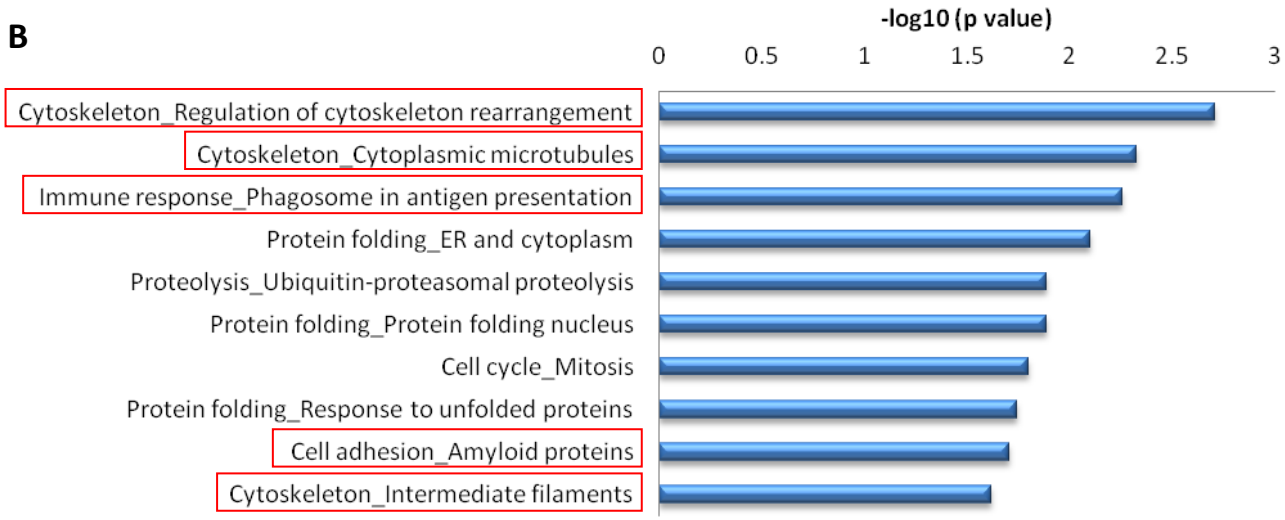

Figure 8 Prostasomal proteins reduced by PTRF expression exhibit significantly different pathways of enrichment. *GeneGo* software was used to identify the top ten significantly enriched processes and pathways (A) Proteins were searched against known biomarkers for enrichment in disease. (B) Enriched cellular processes and pathways were also analysed.

PTRF causes differential Macrophage Migration Inhibitory Factor secretion in prostasomes

While the pathways identified were similar to those in the SILAC study, not all significant proteins were consistently identified. Previously, cytokines such as macrophage migration inhibitory factor (MIF) were found to be significantly different, however, this was not obvious with the data we obtained. Our results only indicated MIF had slightly higher spectral intensities for GFP prostasomes in 3/4 biological samples and was not significantly different. To elucidate whether SILAC or label free methods more accurately reflect prostasome protein quantities, western blots were used. MIF expression was compared in whole cell lysates, prostasomes and prostasome depleted conditioned media. Western blotting results confirmed that MIF was more highly expressed in the PC3:GFP prostasomes (Figure 9) in agreement with the SILAC data. Hence further normalization should be examined for the label-free proteomics work in future.

MIF was present in similar levels in WCL suggesting PTRF regulates secretion. We analysed PTRF depleted conditioned media to determine if PTRF expression affects global release via prostasomes and as a soluble component in conditioned media. Alterations in MIF expression was not restricted to the prostasomes. PTRF prostasome depleted media also showed decreased MIF expression (Figure 9).

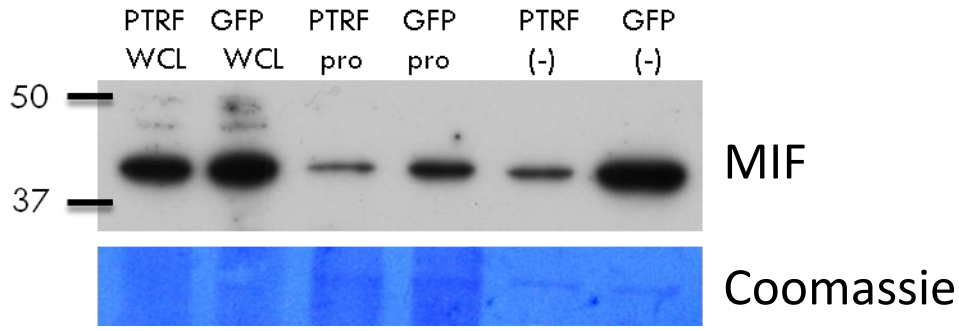

Figure 9 Macrophage Migration Inhibitory Factor (MIF) is differentially secreted. MIF protein expression was analysed by comparing equal total protein (10µg) of whole cell lysates, prostasomes and prostasome depleted conditioned media. MIF showed consistently decreased expression in both prostasomes and exosome depleted media of PC3:PTRF origin which was not seen in whole cell lysates. n=3

MIF secretion occurs through a golgi dependent manner in PC3 cells.

Due to changes in MIF secretion, we investigated the secretory mechanisms involved with PTRF expression. The non classically secreted MIF provides an example to analyse secretion via multiple mechanisms (Rubartelli *et al.*, 1990). Understanding the mechanisms of PTRF-modulated protein secretion may give clues as to how prostasome proteins are packaged and where selected proteins are derived from. MIF lacks the N-terminal specific signalling sequence that facilitates in the transition of proteins to the ER and Golgi (Rubartelli *et al.*, 1990).

Results on MIF localisation in previous reports are contradictory, with some claiming that MIF is solely cytoplasmic while others indicate that there are stores of MIF in the ER (Eickhoff *et al.*, 2001; Wennemuth *et al.*, 2000). Alternate studies indicate that there are stores of MIF within secretory granules and the nucleus (Nishino *et al.*, 1995; Pyle *et al.*, 2003). This may reflect that MIF expression is cell dependent and varies across different cell types. To establish which pathways MIF may be trafficked through, we determined the subcellular localisation of MIF by confocal immunofluorescence microscopy. Cells were fixed and probed for MIF following live uptake of fluorescent tracker dyes. Overall MIF staining showed expression near the plasma membrane and in the peri-nuclear region (Figure 10). No apparent colocalisation was observed with organelle markers for the ER, lysosome and mitochondria.

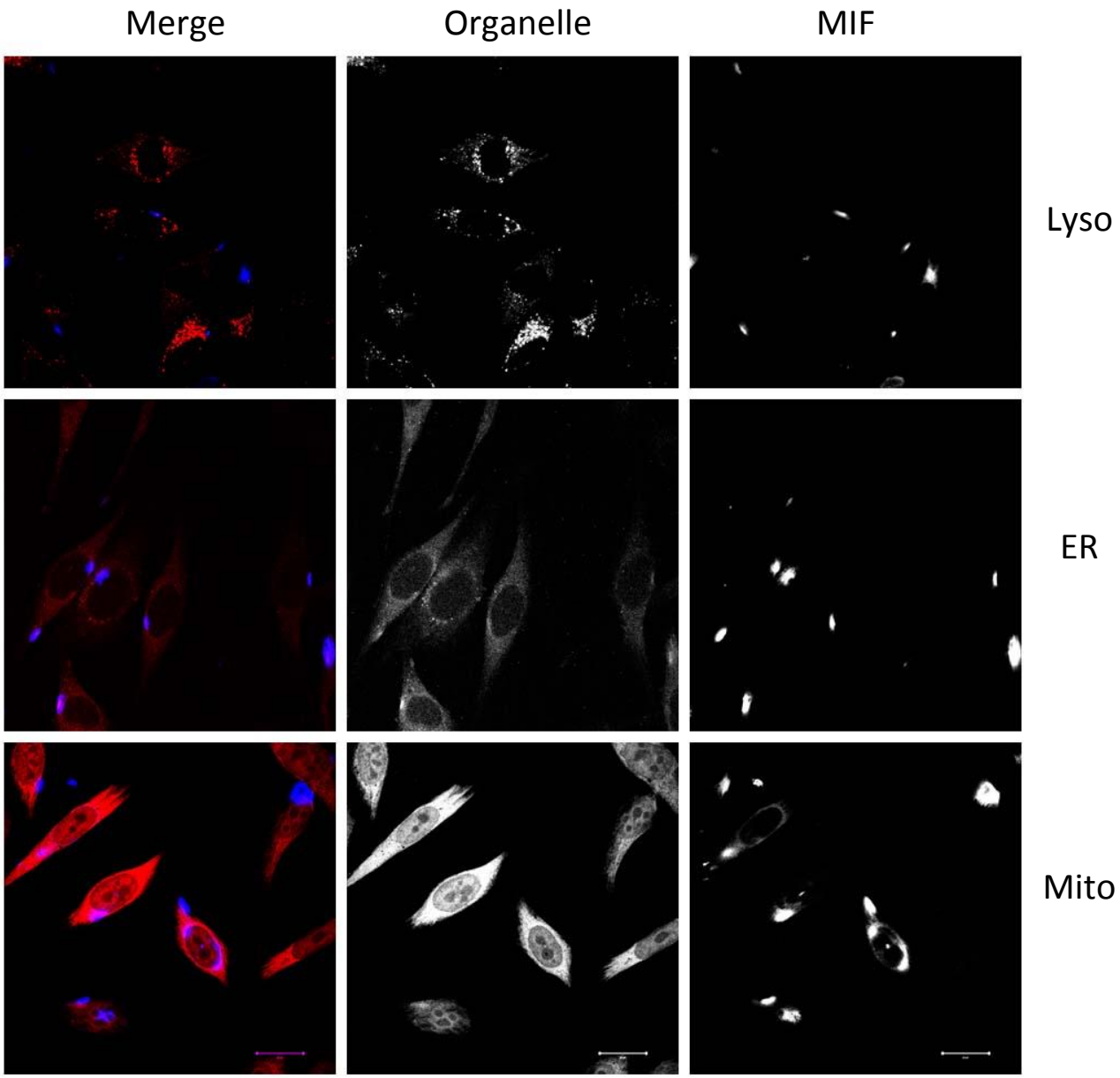

Figure 10 MIF shows no colocalisation with organelle markers in PC3 cells. PC3 cells were plated on coverslips and labelled for organelles by uptake of respective tracker dyes. Cells were co-stained for MIF using anti-MIF antibody. Representative images are shown. Scale bars represent 20µm. Organelle markers are represented as red and MIF as blue. Organelle markers are *Lyso = lysosome tracker, ER = endoplasmic reticulum tracker* and *Mito = mitochondria tracker.*

Next, we investigated the effect of blocking the classical pathway on MIF secretion using Brefeldin A (BFA) which disrupts the membrane recycling out of the ER to the cis/medial Golgi but not back to the ER (Lippincott-Schwartz *et al.*, 1989). Previous reports indicate that BFA redistributes the Golgi (Doms *et al.*, 1989), we therefore used the Golgi marker GRASP65 as a positive control. Since non classical pathways that do not traffic through the Golgi are insensitive to Brefaldin A treatment, we expected no effect on MIF trafficking if its secretion is entirely dependent on non-classical pathways. In BFA-treated PC3 cells, redistribution of GRASP65 was observed (Figure 11) confirming the effect of BFA. In agreement with non-classical secretion, MIF is still concentrated around the plasma membrane in BFA-treated cells (Figure 11) indicating release from organelles before the golgi. MIF had similar expression patterns in both the PC3:GFP and PC3:PTRF cells. Furthermore, BFA treatment showed the same trend for both the PC3:GFP and PC3:PTRF-GFP cells (Figure 11).

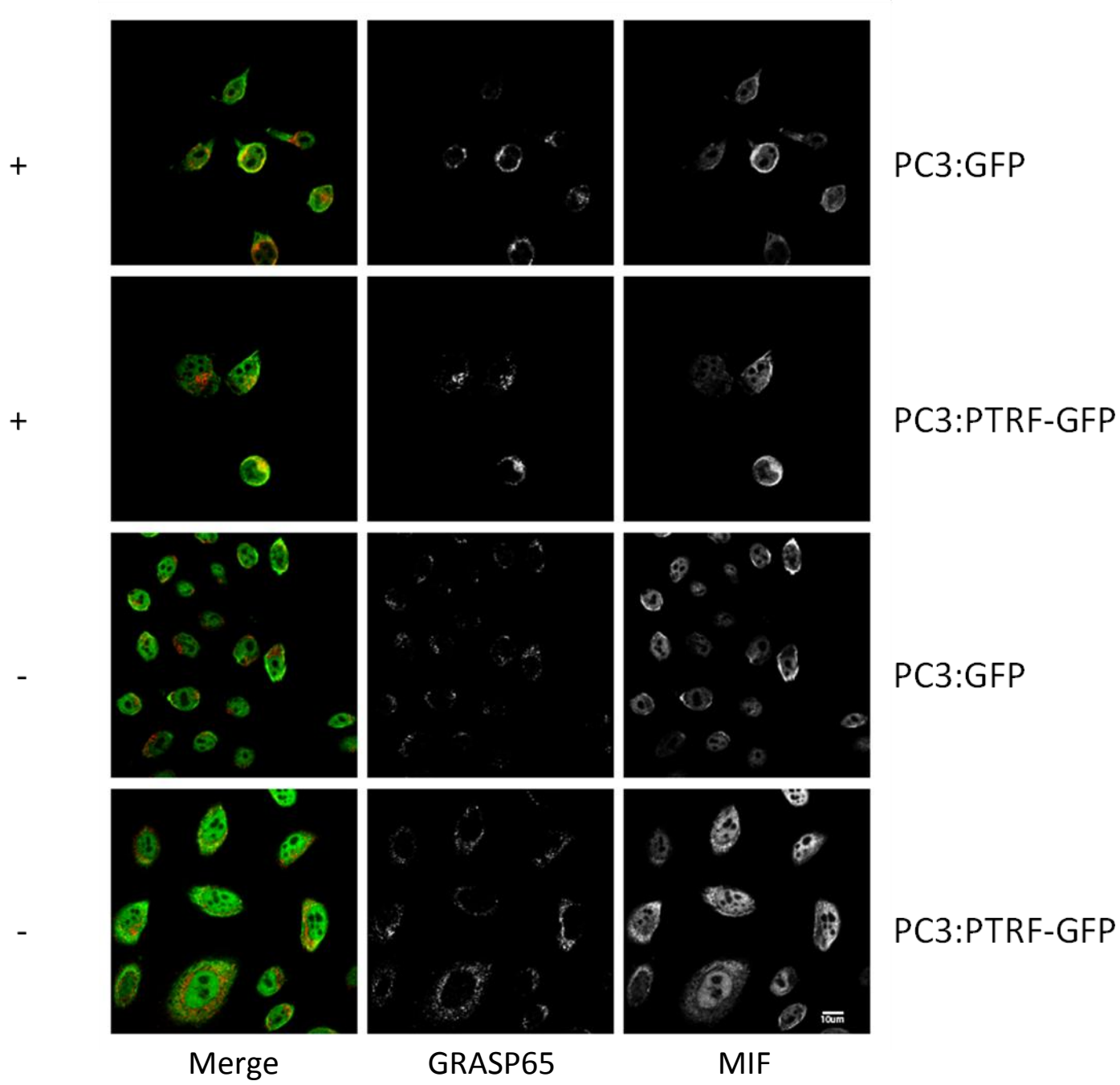

Figure 11 Brefeldin A treatment does not alter MIF distribution. PC3 cells expressing PTRF-GFP or GFP were plated on coverslips and then treated with 0.1ug/mL Brefeldin A (+) or vehicle (-) control for 24 hours. Immunofluorescence was performed to determine the localisation of MIF and the golgi-marker GRASP65. MIF is represented in green while GRASP65 is represented by red. *Scale bar represents 10µm.*

Components within the secreted media may have minor immune modulatory effects that act on monocytes and differentiated macrophages

Given that inflammatory and immune networks were shown to be one of the enriched protein processes, the effects of prostasomes on a candidate immune cell was investigated. Previous studies indicate that conditioned media from tumour cells can contribute to macrophage differentiation (Caras *et al.*, 2011). To elucidate this further, prostasomes were used to treat the human monocytic cell line, THP1, as a model of macrophage differentiation. The vesicular and soluble components of the secretome fraction were added to THP1 cells to address whether the tumour microenvironment and specific components of it can affect the phenotype of THP1 cells and alter macrophage differentiation.

Published conditions were used for in vitro differentiation of THP1 cells to M1 (IFN-γ and LPS), M2a (IL-4 and IL-13) and M2c (IL-10) phenotypes (Caras *et al.*, 2011). As described Caras *et al.*, (2011) these treatments resulted in cells displaying filipodia and becoming adherent (data not shown). Direct addition of prostasomes or prostasome depleted conditioned media to THP1 cells did not alter cellular morphology and adherence to the culture surface after 72 hours. Unlike control differentiated macrophages, the treated cells remained spherical and lacked filipodia, similar to untreated THP1 cells (data not shown).

It was further tested whether prostasomes had an effect on THP-1 differentiation cytokines determined by qPCR. Following the 72 hour differentiation protocol mRNA was extracted from cells. Expression of known markers of macrophage differentiation were investigated with qPCR. Analysis showed that for the cytokines TNF-α, TGF-β,I-L1β, IL-12, IL-6 and IL-23 no significant differences were identified between untreated in comparison to both prostasome and prostasome depleted media treatment groups.

As expected, positive control M1 (LPS and IFN-γ) treatments showed significant differences in gene expression for TNF-α, TGF-β, and IL-6 in comparison to the untreated control. In contrast, IL-12 p40 showed increased expression in M2c (IL-10) differentiated cells that was significantly different to non-treated cells (Figure 12). This suggests that cells were showing some form of phenotypic change in increasing cytokine expression. Differences were not identified for IL-1β and IL-23 in LPS and IFN-γ treated cells as expected for M1 treatments. This limits comparisons being made with prostasome and prostasome depleted media with controls for those particular primers. Increased cytokine expression (TGF-β) was expected between M2a (IL-4 and IL-13) controls and untreated cells, however, no significant differences were identified. The results suggest that differentiation down the M1 or M2c pathway did not occur as they would result in significantly increased expression of TNF-α, TGF-β and IL-6 or IL-12 respectively (Caras *et al*., 2011). Comparisons cannot be drawn between M2a treated cells and those with prostasomes or prostasome depleted media.

As prostasome populations may have alternate effects on polarization from M1 to M2 macrophages, prostasomes and prostasome free media were also added to M1 differentiated cells. Following differentiation of THP1 cells with LPS and IFN-γ for 48 hours, they were subsequently treated with prostasomes or prostasome depleted conditioned media. Here, their morphology remained like M1 macrophages after 48 hours in all treatments (data not shown). As with previous experiments, gene expression was monitored with qPRC. Significant differences were identified in TNF-α expression only in GFP prostasome depleted media ($p<0.05$) (Figure 13). Similar trends of increased TNF-α expression were also evident in GFP prostasomes, however, this was not significant.

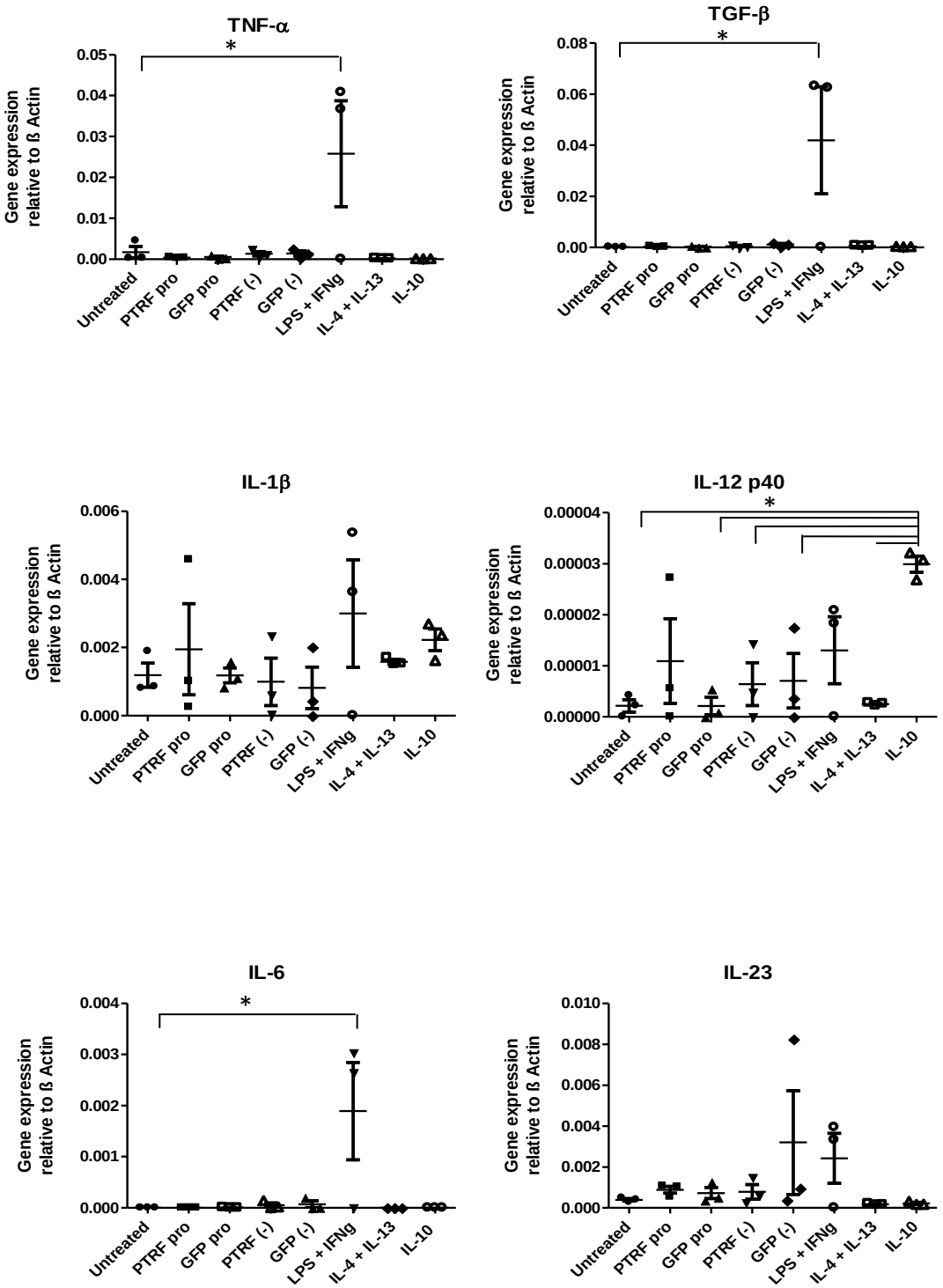

Figure 12 Both prostasomes and prostasome depleted media are unable to significantly alter genes indicative of macrophage differentiation. THP1 cells were treated with control differentiation reagents, prostasomes (pro) or prostasome depleted conditioned media (-). Only control treatments were able to alter cytokine expression measured with qPCR.

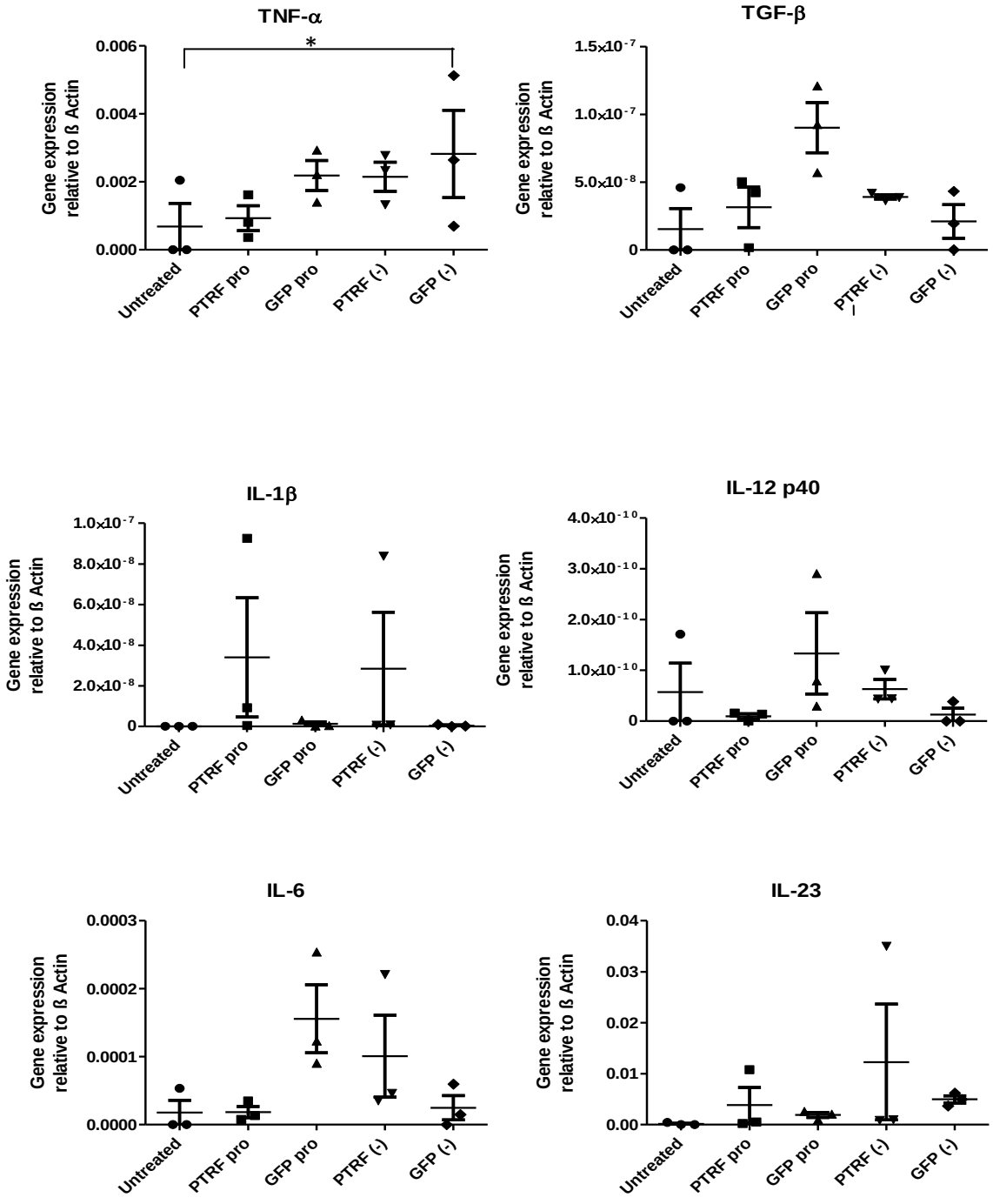

Figure 13 Both prostasomes and prostasome-depleted conditioned media have minimal affects on altering gene expression in differentiated THP1 cells. THP1 cells were first differentiated to M1 macrophages using LPS and IFN-γ then treated with prostasomes or prostasome-depleted condition media for 2 days. Expression of the indicated cytokines were assayed by qPCR. Only TNF-α showed a significant change in expression in GFP (-) in comparison to the untreated control ($p<0.05$). n=3

To determine whether minimal changes in gene expression were specific to cytokines, CD14 expression was also monitored. CD14 is a membrane receptor that has increased expression associated with M1 macrophage differentiation (Schraufstatter *et al.*, 2012). While not significant, there appeared to be a trend of increased CD14 mRNA expression in treatment conditions in comparison to untreated cells. In THP1 differentiation experiments, this trend also appeared in the LPS and IFN-γ treated cells but not the IL-10 or IL-4 and IL-13 treatment groups (Figure 14).

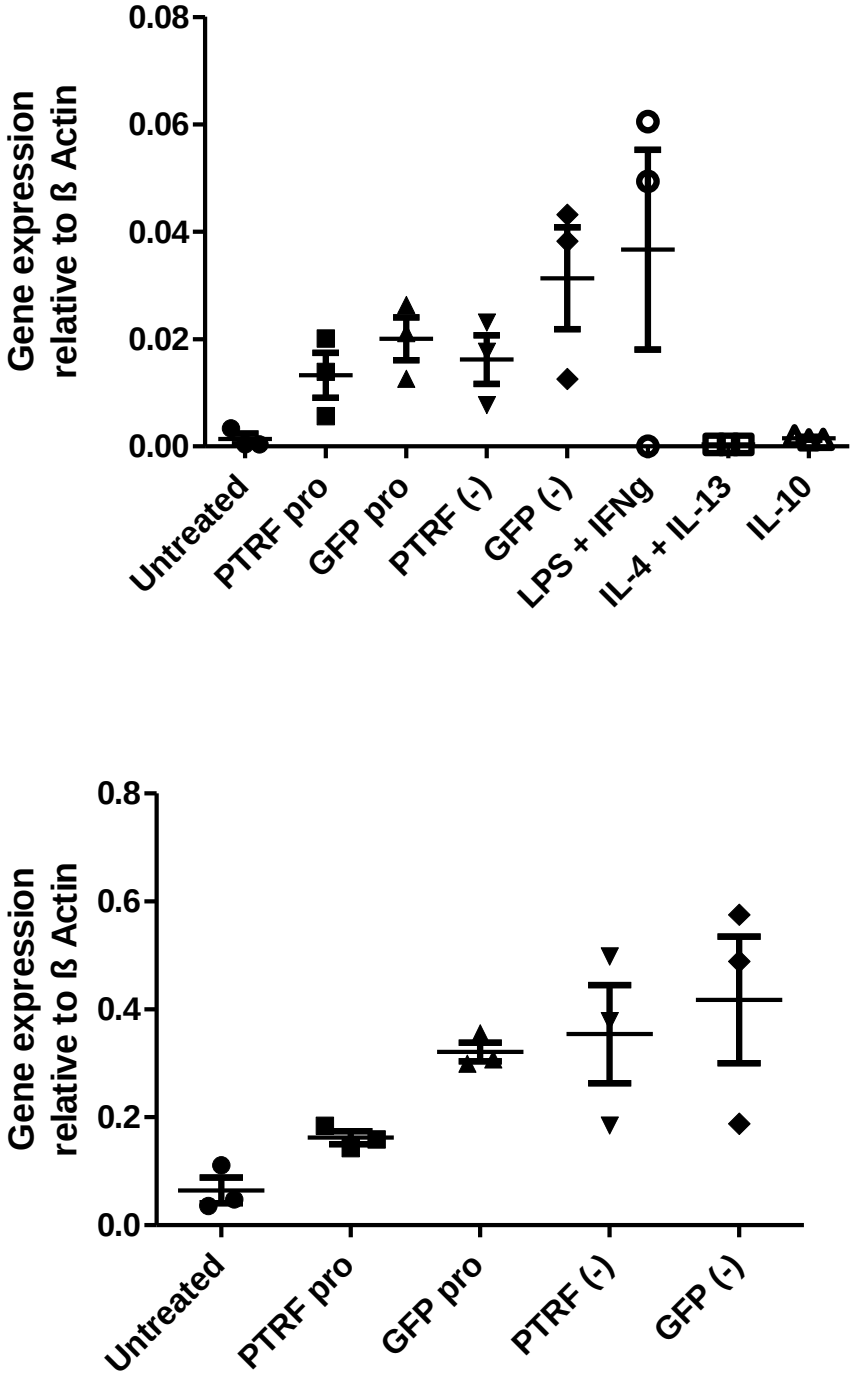

Figure 14 The membrane receptor CD14 showed no significant difference in gene expression following treatment with prostasomes or prostasome depleted media. Treatment of (A) THP1 cells and (B) M1 differentiated macrophages with prostasome and prostasome-depeleted conditioned media was performed as for Figures 10 and 11 respectively. n=3.

Discussion

The findings presented here indicate that the introduction of the PTRF gene reduced the size, concentration and sub-proteome of prostasomes released from PC3 prostate cancer cells. While immune modulatory proteins such as MIF were differentially regulated, these may act through pathways independent of macrophage differentiation.

Pathway analysis of differentially secreted proteins in prostasomes identified lymphatic metastasis as one of the possible diseases. The lymph nodes are one of the primary sites of prostate cancer metastasis (Wu *et al.*, 2011). This indicates that introduction of the PTRF gene may significantly attenuate characteristics of prostate cancer and reduce it to a less aggressive form. This is consistent with recent *in vivo* work completed in our lab that shows generation of tumours in mice from PC3:PTRF cells show less lymphatic metastasis in comparison to PC3:GFP tumours (unpublished).

The average size of prostasomes as determined using dynamic light scattering experiments fits well within the 40-500nm accepted value of prostasome size (Utleg *et al.*, 2003). While particles were detected outside this range, this only comprises 4.7% and 5.2% for PC3:PTRF and PC3:GFP samples respectively. These outliers ranged from 3.5-5.5µm and may correspond to the extremely large tumour-derived microvesicles (TMV) recently described as oncosomes (Di Vizio *et al.*). These are believed to be a common feature in aggressive prostate cancer, however, our study suggests these large oncosomes represent a minor component of secreted vesicles. Unlike prior analysis using Fluorescent Activated Cell Sorting or Electron Microscopy, samples do not need to be fixed or treated with antibodies for detection by dynamic light scattering (Aalberts *et al.*, 2011; Carlsson *et al.*, 2003). As this method of size detection only requires the sample to be suspended in a liquid, size may more accurately reflect the physiological sizes of the vesicles.

Changes in either the morphology, size or concentration in this instance are a direct effect of PTRF expression. Although the direct mechanisms for prostasome or exosome packaging are not clearly established, current literature suggests that cholesterol may play a role in prostasome release. Cholesterol forms membrane microdomains, termed lipid rafts, which are thought to mediate lateral protein segregation and interactions within cellular membranes. Lipid rafts also mediate membrane trafficking. Depletion of cholesterol from PC3 cells significantly decreased the number of prostasomes released (Llorente *et al.*, 2007). Previous studies from our lab suggests that PTRF specifically alters lipid raft cholesterol without affecting the total cellular cholesterol levels(Inder *et al.*, 2012). Taken together, reduced cholesterol in lipid raft fractions may lead to the decreased prostasome release from PTRF:PC3 cells. Depleting total cholesterol in PC3:PTRF and PC3:PTRF-GFP cells may aid in establishing whether this occurs solely through PTRF dependent effects on cholesterol or alternate mechanisms.

Prostasomes are enriched in cholesterol displaying a 2 fold increase in comparison to the cell membrane (Arienti *et al.*, 1998). High cholesterol levels alter the membrane dynamics, forming a stable structure of highly ordered lipids (Arvidson *et al.*, 1989). If prostasomes contain an altered cholesterol distribution, this may alter the type of proteins transported. Due to the inherent nature of cholesterol to retain or exclude cellular proteins, preferential packaging may be implored (Epand, 2006). Acylation, glycosylphosphatidylinositol linkage or cholesterol attachment is required for proteins to remain within cholesterol rich regions such as lipid rafts (Karpen *et al.*, 2001; Morandat *et al.*, 2002).

Consistent with previous proteomic profiling for PTRF effects on PC3 prostasomes (Inder *et al.*, 2012) the current prostasome analysis revealed significant alterations in cytoskeletal

remodelling pathways. Cell adhesion, cytoskeleton remodeling, cytoskeletal rearrangement, cell adhesion and tissue degradation are all processes required for metastasis. Within the PC3 cell, PTRF reduced the metastatic ability by altering both the directional migration of cells and the number of cellular protrusions (Hill *et al.*, 2012). PC3-released prostasomes may act on the surrounding tissue micro-environment to aid cancer cell invasion. The relative cell-intrinsic and stromal-remodelling roles of PTRF should be assessed in future experiments by examining the prostasome or conditioned media effects on the cytoskeleton and migration of other prostate cancer cells (for example, LNCaP).

Immune modulation was also predicted to be a process altered by PTRF in PC3 prostasomes. We examined one aspect of immune modulation, namely the differentiation and polarization of macrophages, based on previous results reporting tumour exosome-mediated macrophage differentiation (Al-Nedawi *et al.*, 2009b). While the control cytokine treatments induced macrophage differentiation to M1 and M2, no significant effect was observed with either prostasomes or prostasome-depleted conditioned media. A trend towards increased TNF-α expression in M1 macrophages when treated with GFP conditioned media and possibly prostasomes suggest that while cells may not be trans-differentiating, components in the conditioned media have some effect on macrophage cytokine expression. TNF-α is a pro-inflammatory cytokine and is required for macrophage maintenance (Popov *et al.*, 2006). Increased levels may suggest conditioned media maintains resident macrophages in the tumour (Beyer *et al.*, 2012).

As previous studies suggest that tumour cells are able to induce macrophage differentiation, this could indicate that components in both the conditioned media and prostasomes are required together. Studies that showed macrophage differentiation used total conditioned

media as opposed to prostasome depleted media (Caras *et al.*, 2011). This may also depend on the tumour type in question. Previous attempts at macrophage differentiation using conditioned media have been described for colorectal, laryngeal cancer, breast cancer and pancreatic cancer (Caras *et al.*, 2011; Solinas *et al.*, 2010; Stewart *et al.*, 2012). This may also be tumour or cell specific, whereby pancreatic cancer models show that amongst aggressive cell lines, only some induce macrophage differentiation (Solinas *et al.*, 2010). Furthermore, prostasomes or conditioned media may still affect primary monocytes or tissue macrophages compared to the cell line used here.

Alternate pathways give an indication that proteins packaged in prostasomes are highly related to those found in lipid rafts. While mechanisms responsible for sorting proteins into the two compartments is not completely understood, it is suggested that proteins found within exosomes may be derived from rafts (Chen *et al.*, 2011) (Calzolari *et al.*, 2006). As PTRF has been shown to alter the raft dynamics this may reflect that PTRF attenuates gene expression in a manner that affects both prostasomes and rafts specifically (Inder *et al.*, 2012; Liu and Pilch, 2008).

To begin to decipher the secretory pathway involved in PTRF-mediated prostasome modulation, we examined one candidate protein identified in mass spectrometry data, MIF. MIF plays a role in macrophage migration (Gregory *et al.*, 2006) and has been suggested as a potential biomarker for prostate cancer progression (Meyer-Siegler *et al.*, 2002). This is consistent with a previous study that showed LNCaP or DU145 prostate cancer cells also have upregulation of MIF secretion in relation to benign cancer cells (Meyer-Siegler *et al.*, 2006).

PTRF-mediated down-regulation of MIF secretion was validated by western blot (Figure 5), which also showed similar total cellular levels of MIF in GFP and PTRF-GFP PC3 cells, suggesting the main effect of PTRF is on the secretory pathway. Immunofluorescence experiments were performed to determine the subcellular location of MIF in PC3 cells. Secretion of MIF is thought to occur via a non-classical pathway in THP1 cells (Flieger *et al.*, 2003). Our data suggests that MIF is present in the nucleus and cytoplasm but absent in the Golgi and supports the progression of MIF directly from the nucleus to the cytoplasm or membrane in PC3 cells.

Further evidence was obtained using the Golgi inhibitor Brefeldin A. While cells in the treatment conditions looked morphologically different with re-distribution of Golgi and changed cell shape, MIF localisation was not significantly different suggesting that the non-classical secretion mechanism is the only pathway in operation for MIF secretion in PC3 cells.

Since we hypothesized differential secretion of MIF, the localization of MIF was expected to be different in cells expressing PTRF. However, this was not apparent in the current immunofluorescence results (Figure 11). The time and space resolution of confocal microscopy may introduce technical limitations for these experiments. While a lack of differences in localisation may indicate that packaging is consistent, if packaging occurs transiently, this may not be observable. Likewise, differences in the proportion of MIF that occupies each prostasome vesicle cannot be accurately observed with microscopy. Further quantification of MIF protein normalised to prostasome number could now be carried out given the identification of prostasome release concentrations. In future, colocalisation should also be repeated with a known prostasome or exosome marker. Alternatively,

prostasomes collected from BFA treated cells could further verify that the proportion of MIF in secreted prostasomes is not altered by blocking classical secretion.

The non-classical secretion pathway identified may take one of two routes. MIF was found in both prostasomes and prostasome free fractions indicating there are two mechanisms of non-classical release. As the total MIF levels were both changed in the same direction upon introduction of PTRF, this may indicate that PTRF acts at an early stage to regulate release consistently.

The most significantly reduced protein in our mass spectrometry data is charged multivesicular body protein 5 (CHMP5). CHMP5 affects multivesicular body protein sorting and degradation (Shim *et al.*, 2006). Silencing CHMP5 reduces protein degradation and progression of vesicles to the lysosome (Ward *et al.*, 2005). Synonymous with this, CHMP5 depletion increased the number of viral vectors released from the cell. Knockouts for CHMP5 also result in larger late endosomal compartments forming that are abundant in internal vesicles (Shim *et al.*, 2006). This could potentially explain differences identified in our prostasome concentration analysis. Our data show that only prostasomes from control GFP PC3 cells contained CHMP5 indicating that PTRF may inhibit CHMP5 expression or function resulting in the lower concentration of secreted prostasomes. Bulk MVB release is unlikely to be affected since marker proteins CD63 and Alix were not significantly altered (Shim *et al.*, 2006). Therefore, CHMP5 may be responsible for sorting of specific prostasome components. Knockdown of CHMP5 in PC3 cells followed by sizing and proteomics of prostasomes will provide further information on the role of CHMP5.

Conclusions and future directions

This study established PTRF alters the size, concentration and specific proteomic contents of PC3 prostasomes, but PC3 prostasomes were unable to differentiate or transdifferentiate macrophages. Western blot validation of MIF secretion suggest that the SILAC proteomics quantitation is more accurate. Future work should investigate alternate normalisation methods for label-free quantitative proteomics. Nonetheless, proteins identified within prostasomes provide further clues as to how PTRF acts to selectively package proteins. Non-classically secreted cytokines such as MIF provide an example of proteins that evade golgi processing but are released through prostasomes. As this is modulated by PTRF, caveolae or associated lipid rafts must play a role in altering a component of that pathway, potentially through CHMP5.

References

Aalberts, M., van Dissel-Emiliani, F.M.F., van Adrichem, N.P.H., van Wijnen, M., Wauben, M.H.M., Stout, T.A.E., and Stoorvogel, W. (2011). Identification of Distinct Populations of Prostasomes That Differentially Express Prostate Stem Cell Antigen, Annexin A1, and GLIPR2 in Humans1. Biology of Reproduction *86*, 82.

Abrahams, V.M., Straszewski, S.L., Kamsteeg, M., Hanczaruk, B., Schwartz, P.E., Rutherford, T.J., and Mor, G. (2003). Epithelial ovarian cancer cells secrete functional Fas ligand. Cancer Res *63*, 5573-5581.

Al-Nedawi, K., Meehan, B., Kerbel, R.S., Allison, A.C., and Rak, J. (2009a). Endothelial expression of autocrine VEGF upon the uptake of tumor-derived microvesicles containing oncogenic EGFR. Proceedings of the National Academy of Sciences of the United States of America *106*, 3794-3799.

Al-Nedawi, K., Meehan, B., and Rak, J. (2009b). Microvesicles Messengers and mediators of tumor progression. Cell cycle (Georgetown, Tex) *8*, 2014-2018.

Arienti, G., Carlini, E., Polci, A., Cosmi, E.V., and Palmerini, C.A. (1998). Fatty Acid Pattern of Human Prostasome Lipid. Archives of Biochemistry and Biophysics *358*, 391-395.

Arvidson, G., Ronquist, G., Wikander, G., and Öjteg, A.-C. (1989). Human prostasome membranes exhibit very high cholesterol/phospholipid ratios yielding high molecular ordering. Biochimica et Biophysica Acta (BBA) - Biomembranes *984*, 167-173.

Aung, C.S., Hill, M.M., Bastiani, M., Parton, R.G., and Parat, M.-O. (2011). PTRF–cavin-1 expression decreases the migration of PC3 prostate cancer cells: Role of matrix metalloprotease 9. European Journal of Cell Biology *90*, 136-142.

Auvinen, E., Carpen, O., Korpela, T., Ronty, M., Vaheri, A., and Tarkkanen, J. (2012). Altered Expression of ezrin, E-Cadherin and beta-Catenin in Cervical Neoplasia. Neoplasma.

Basch, E., Oliver, T.K., Vickers, A., Thompson, I., Kantoff, P., Parnes, H., Loblaw, D.A., Roth, B., Williams, J., and Nam, R.K. (2012). Screening for Prostate Cancer With Prostate-Specific Antigen Testing: American Society of Clinical Oncology Provisional Clinical Opinion. Journal of Clinical Oncology *30*, 3020-3025.

Bastiani, M., and Parton, R.G. (2010). Caveolae at a glance. Journal of cell science *123*, 3831-3836.

Beyer, M., Mallmann, M.R., Xue, J., Staratschek-Jox, A., Vorholt, D., Krebs, W., Sommer, D., Sander, J., Mertens, C., Nino-Castro, A*., et al.* (2012). High-Resolution Transcriptome of Human Macrophages. PLoS ONE *7*, e45466.

Biswas, S.K., and Mantovani, A. (2010). Macrophage plasticity and interaction with lymphocyte subsets: cancer as a paradigm. Nat Immunol *11*, 889-896.

Buhtoiarov, I.N., Sondel, P.M., Wigginton, J.M., Buhtoiarova, T.N., Yanke, E.M., Mahvi, D.A., and Rakhmilevich, A.L. (2011). Anti-tumour synergy of cytotoxic chemotherapy and anti-

CD40 plus CpG-ODN immunotherapy through repolarization of tumour-associated macrophages. Immunology *132*, 226-239.

Burkard, T.R., Planyavsky, M., Kaupe, I., Breitwieser, F.P., Burckstummer, T., Bennett, K.L., Superti-Furga, G., and Colinge, J. (2011). Initial characterization of the human central proteome. BMC systems biology *5*, 17.

Cairns, D.A., Thompson, D., Perkins, D.N., Stanley, A.J., Selby, P.J., and Banks, R.E. (2008). Proteomic profiling using mass spectrometry--does normalising by total ion current potentially mask some biological differences? Proteomics *8*, 21-27.

Calzolari, A., Raggi, C., Deaglio, S., Sposi, N.M., Stafsnes, M., Fecchi, K., Parolini, I., Malavasi, F., Peschle, C., Sargiacomo, M*., et al.* (2006). TfR2 localizes in lipid raft domains and is released in exosomes to activate signal transduction along the MAPK pathway. Journal of cell science *119*, 4486-4498.

Caras, I., Tucureanu, C., Lerescu, L., Pitica, R., Melinceanu, L., Neagu, S., and Salageanu, A. (2011). Influence of tumor cell culture supernatants on macrophage functional polarization: in vitro models of macrophage-tumor environment interaction. Tumori *97*, 647-654.

Carlsson, L., Nilsson, O., Larsson, A., Stridsberg, M., Sahlén, G., and Ronquist, G. (2003). Characteristics of human prostasomes isolated from three different sources. The Prostate *54*, 322-330.

Chen, T., Guo, J., Yang, M., Zhu, X., and Cao, X. (2011). Chemokine-Containing Exosomes Are Released from Heat-Stressed Tumor Cells via Lipid Raft-Dependent Pathway and Act as Efficient Tumor Vaccine. The Journal of Immunology *186*, 2219-2228.

Corn, P.G., and Thompson, T.C. (2010). Identification of a novel prostate cancer biomarker, caveolin-1: Implications and potential clinical benefit. Cancer management and research *2*, 111-122.

Davidsson, S., Ohlson, A.-L., Andersson, S.-O., Fall, K., Meisner, A., Fiorentino, M., Andren, O., and Rider, J.R. (2012). CD4 helper T cells, CD8 cytotoxic T cells, and FOXP3+ regulatory T cells with respect to lethal prostate cancer. Mod Pathol.

Di Vizio, D., Morello, M., Dudley, A.C., Schow, P.W., Adam, R.M., Morley, S., Mulholland, D., Rotinen, M., Hager, M.H., Insabato, L*., et al.* Large Oncosomes in Human Prostate Cancer Tissues and in the Circulation of Mice with Metastatic Disease. The American Journal of Pathology.

Doms, R.W., Russ, G., and Yewdell, J.W. (1989). Brefeldin A redistributes resident and itinerant Golgi proteins to the endoplasmic reticulum. The Journal of cell biology *109*, 61-72.

Donatello, S., Babina, I.S., Hazelwood, L.D., Hill, A.D., Nabi, I.R., and Hopkins, A.M. (2012). Lipid Raft Association Restricts CD44-Ezrin Interaction and Promotion of Breast Cancer Cell Migration. Am J Pathol.

Donkor, M.K., Sarkar, A., Savage, P.A., Franklin, R.A., Johnson, L.K., Jungbluth, A.A., Allison, J.P., and Li, M.O. (2011). T cell surveillance of oncogene-induced prostate cancer is impeded by T cell-derived TGF-beta1 cytokine. Immunity *35*, 123-134.

Duijvesz, D., Luider, T., Bangma, C.H., and Jenster, G. (2011). Exosomes as Biomarker Treasure Chests for Prostate Cancer. European Urology *59*, 823-831.

Eickhoff, R., Wilhelm, B., Renneberg, H., Wennemuth, G., Bacher, M., Linder, D., Bucala, R., Seitz, J., and Meinhardt, A. (2001). Purification and Characterization of Macrophage Migration Inhibitory Factor as a Secretory Protein from Rat Epididymis: Evidences for Alternative Release and Transfer to Spermatozoa. Molecular Medicine *7*, 27-35.

Epand, R.M. (2006). Cholesterol and the interaction of proteins with membrane domains. Progress in Lipid Research *45*, 279-294.

Flieger, O., Engling, A., Bucala, R., Lue, H., Nickel, W., and Bernhagen, J. (2003). Regulated secretion of macrophage migration inhibitory factor is mediated by a non-classical pathway involving an ABC transporter. FEBS Lett *551*, 78-86.

Grange, C., Tapparo, M., Collino, F., Vitillo, L., Damasco, C., Deregibus, M.C., Tetta, C., Bussolati, B., and Camussi, G. (2011). Microvesicles released from human renal cancer stem cells stimulate angiogenesis and formation of lung premetastatic niche. Cancer Res *71*, 5346-5356.

Gregory, J.L., Morand, E.F., McKeown, S.J., Ralph, J.A., Hall, P., Yang, Y.H., McColl, S.R., and Hickey, M.J. (2006). Macrophage migration inhibitory factor induces macrophage recruitment via CC chemokine ligand 2. Journal of immunology (Baltimore, Md : 1950) *177*, 8072-8079.

Griffin, N.M., Yu, J., Long, F., Oh, P., Shore, S., Li, Y., Koziol, J.A., and Schnitzer, J.E. (2010). Label-free, normalized quantification of complex mass spectrometry data for proteomic analysis. Nat Biotech *28*, 83-89.

Gurtner, G.C., Werner, S., Barrandon, Y., and Longaker, M.T. (2008). Wound repair and regeneration. Nature *453*, 314-321.

Hao, S., Ye, Z., Li, F., Meng, Q., Qureshi, M., Yang, J., and Xiang, J. (2006). Epigenetic transfer of metastatic activity by uptake of highly metastatic B16 melanoma cell-released exosomes. Experimental oncology *28*, 126-131.

Hill, M.M., Bastiani, M., Luetterforst, R., Kirkham, M., Kirkham, A., Nixon, S.J., Walser, P., Abankwa, D., Oorschot, V.M.J., Martin, S.*, et al.* (2008). PTRF-Cavin, a Conserved Cytoplasmic Protein Required for Caveola Formation and Function. Cell *132*, 113-124.

Hill, M.M., Daud, N.H., Aung, C.S., Loo, D., Martin, S., Murphy, S., Black, D.M., Barry, R., Simpson, F., Liu, L.*, et al.* (2012). Co-Regulation of Cell Polarization and Migration by Caveolar Proteins PTRF/Cavin-1 and Caveolin-1. PLoS ONE *7*, e43041.

Hong, B.S., Cho, J.H., Kim, H., Choi, E.J., Rho, S., Kim, J., Kim, J.H., Choi, D.S., Kim, Y.K., Hwang, D*., et al.* (2009). Colorectal cancer cell-derived microvesicles are enriched in cell cycle-related mRNAs that promote proliferation of endothelial cells. BMC genomics *10*, 556.

Hosseini-Beheshti, E., Pham, S., Adomat, H., Li, N., and Guns, E.S. (2012). Exosomes as Biomarker Enriched Microvesicles: Characterization of Exosomal Proteins derived from a Panel of Prostate Cell Lines with distinct AR phenotypes. Molecular & Cellular Proteomics.

Iero, M., Valenti, R., Huber, V., Filipazzi, P., Parmiani, G., Fais, S., and Rivoltini, L. (2008). Tumour-released exosomes and their implications in cancer immunity. Cell death and differentiation *15*, 80-88.

Inder, K.L., Zheng, Y.Z., Davis, M.J., Moon, H., Loo, D., Nguyen, H., Clements, J.A., Parton, R.G., Foster, L.J., and Hill, M.M. (2012). Expression of PTRF in PC-3 Cells Modulates Cholesterol Dynamics and the Actin Cytoskeleton Impacting Secretion Pathways. Molecular & Cellular Proteomics *11*.

Ishihama, Y., Oda, Y., Tabata, T., Sato, T., Nagasu, T., Rappsilber, J., and Mann, M. (2005). Exponentially Modified Protein Abundance Index (emPAI) for Estimation of Absolute Protein Amount in Proteomics by the Number of Sequenced Peptides per Protein. Molecular & Cellular Proteomics *4*, 1265-1272.

Janji, B., Giganti, A., De Corte, V., Catillon, M., Bruyneel, E., Lentz, D., Plastino, J., Gettemans, J., and Friederich, E. (2006). Phosphorylation on Ser5 increases the F-actin-binding activity of L-plastin and promotes its targeting to sites of actin assembly in cells. Journal of cell science *119*, 1947-1960.

Jemal, A., Bray, F., Center, M.M., Ferlay, J., Ward, E., and Forman, D. (2011). Global cancer statistics. CA Cancer J Clin *61*, 69-90.

Karpen, H.E., Bukowski, J.T., Hughes, T., Gratton, J.-P., Sessa, W.C., and Gailani, M.R. (2001). The Sonic Hedgehog Receptor Patched Associates with Caveolin-1 in Cholesterol-rich Microdomains of the Plasma Membrane. Journal of Biological Chemistry *276*, 19503-19511.

Lin, E.Y., Nguyen, A.V., Russell, R.G., and Pollard, J.W. (2001). Colony-Stimulating Factor 1 Promotes Progression of Mammary Tumors to Malignancy. The Journal of Experimental Medicine *193*, 727-740.

Lippincott-Schwartz, J., Yuan, L.C., Bonifacino, J.S., and Klausner, R.D. (1989). Rapid redistribution of Golgi proteins into the ER in cells treated with brefeldin A: evidence for membrane cycling from Golgi to ER. Cell *56*, 801-813.

Liu, L., and Pilch, P.F. (2008). A critical role of cavin (polymerase I and transcript release factor) in caveolae formation and organization. The Journal of biological chemistry *283*, 4314-4322.

Llorente, A., van Deurs, B., and Sandvig, K. (2007). Cholesterol regulates prostasome release from secretory lysosomes in PC-3 human prostate cancer cells. European Journal of Cell Biology *86*, 405-415.

Mantovani, A., Sica, A., and Locati, M. (2005). Macrophage Polarization Comes of Age. Immunity *23*, 344-346.

Mantovani, A., Sica, A., Sozzani, S., Allavena, P., Vecchi, A., and Locati, M. (2004). The chemokine system in diverse forms of macrophage activation and polarization. Trends Immunol *25*, 677-686.

Mantovani, A., Sozzani, S., Locati, M., Allavena, P., and Sica, A. (2002). Macrophage polarization: tumor-associated macrophages as a paradigm for polarized M2 mononuclear phagocytes. Trends in Immunology *23*, 549-555.

Martin-Serrano, J., Yarovoy, A., Perez-Caballero, D., and Bieniasz, P.D. (2003). Divergent retroviral late-budding domains recruit vacuolar protein sorting factors by using alternative adaptor proteins. Proceedings of the National Academy of Sciences of the United States of America *100*, 12414-12419.

Mathivanan, S., and Simpson, R.J. (2009). ExoCarta: A compendium of exosomal proteins and RNA. Proteomics *9*, 4997-5000.

Meyer-Siegler, K.L., Bellino, M.A., and Tannenbaum, M. (2002). Macrophage migration inhibitory factor evaluation compared with prostate specific antigen as a biomarker in patients with prostate carcinoma. Cancer *94*, 1449-1456.

Meyer-Siegler, K.L., Iczkowski, K.A., Leng, L., Bucala, R., and Vera, P.L. (2006). Inhibition of macrophage migration inhibitory factor or its receptor (CD74) attenuates growth and invasion of DU-145 prostate cancer cells. Journal of immunology (Baltimore, Md : 1950) *177*, 8730-8739.

Milsom, C., Yu, J., May, L., Meehan, B., Magnus, N., Al-Nedawi, K., Luyendyk, J., Weitz, J., Klement, P., Broze, G.*, et al.* (2007). The role of tumor-and host-related tissue factor pools in oncogene-driven tumor progression. Thrombosis research *120 Suppl 2*, S82-91.

Morandat, S., Bortolato, M., and Roux, B. (2002). Cholesterol-dependent insertion of glycosylphosphatidylinositol-anchored enzyme. Biochimica et Biophysica Acta - Biomembranes *1564*, 473-478.

Mosser, D.M., and Edwards, J.P. (2008). Exploring the full spectrum of macrophage activation. Nat Rev Immunol *8*, 958-969.

Murray, P.J., and Wynn, T.A. (2011). Protective and pathogenic functions of macrophage subsets. Nat Rev Immunol *11*, 723-737.

Nishino, T., Bernhagen, J., Shiiki, H., Calandra, T., Dohi, K., and Bucala, R. (1995). Localization of macrophage migration inhibitory factor (MIF) to secretory granules within the corticotrophic and thyrotrophic cells of the pituitary gland. Molecular medicine (Cambridge, Mass) *1*, 781-788.

Ong, S.-E., Blagoev, B., Kratchmarova, I., Kristensen, D.B., Steen, H., Pandey, A., and Mann, M. (2002). Stable Isotope Labeling by Amino Acids in Cell Culture, SILAC, as a Simple and Accurate Approach to Expression Proteomics. Molecular & Cellular Proteomics *1*, 376-386.

Pello, O.M., De Pizzol, M., Mirolo, M., Soucek, L., Zammataro, L., Amabile, A., Doni, A., Nebuloni, M., Swigart, L.B., Evan, G.I.*, et al.* (2012). Role of c-MYC in alternative activation of human macrophages and tumor-associated macrophage biology. Blood *119*, 411-421.

Popov, A., Abdullah, Z., Wickenhauser, C., Saric, T., Driesen, J., Hanisch, F.G., Domann, E., Raven, E.L., Dehus, O., Hermann, C.*, et al.* (2006). Indoleamine 2,3-dioxygenase-expressing dendritic cells form suppurative granulomas following Listeria monocytogenes infection. The Journal of clinical investigation *116*, 3160-3170.

Pyle, M., Korbonits, M., Gueorguiev, M., Jordan, S., Kola, B., Morris, D., Meinhardt, A., Powell, M., Claret, F., Zhang, Q.*, et al.* (2003). Macrophage migration inhibitory factor expression is increased in pituitary adenoma cell nuclei. Journal of Endocrinology *176*, 103-110.

Redente, E.F., Dwyer-Nield, L.D., Merrick, D.T., Raina, K., Agarwal, R., Pao, W., Rice, P.L., Shroyer, K.R., and Malkinson, A.M. (2010). Tumor Progression Stage and Anatomical Site Regulate Tumor-Associated Macrophage and Bone Marrow-Derived Monocyte Polarization. The American Journal of Pathology *176*, 2972-2985.

Rubartelli, A., Cozzolino, F., Talio, M., and Sitia, R. (1990). A novel secretory pathway for interleukin-1β, a protein lacking a signal sequence. EMBO Journal *9*, 1503-1510.

Scarpino, S., Stoppacciaro, A., Ballerini, F., Marchesi, M., Prat, M., Stella, M.C., Sozzani, S., Allavena, P., Mantovani, A., and Ruco, L.P. (2000). Papillary carcinoma of the thyroid: hepatocyte growth factor (HGF) stimulates tumor cells to release chemokines active in recruiting dendritic cells. Am J Pathol *156*, 831-837.

Schraufstatter, I.U., Zhao, M., Khaldoyanidi, S.K., and Discipio, R.G. (2012). The chemokine CCL18 causes maturation of cultured monocytes to macrophages in the M2 spectrum. Immunology *135*, 287-298.

Shim, J.H., Xiao, C., Hayden, M.S., Lee, K.Y., Trombetta, E.S., Pypaert, M., Nara, A., Yoshimori, T., Wilm, B., Erdjument-Bromage, H.*, et al.* (2006). CHMP5 is essential for late endosome function and down-regulation of receptor signaling during mouse embryogenesis. The Journal of cell biology *172*, 1045-1056.

Sidhu, S.S., Mengistab, A.T., Tauscher, A.N., LaVail, J., and Basbaum, C. (2004). The microvesicle as a vehicle for EMMPRIN in tumor-stromal interactions. Oncogene *23*, 956-963.

Simons, K., and Ikonen, E. (1997). Functional rafts in cell membranes. Nature *387*, 569-572.

Solinas, G., Schiarea, S., Liguori, M., Fabbri, M., Pesce, S., Zammataro, L., Pasqualini, F., Nebuloni, M., Chiabrando, C., Mantovani, A.*, et al.* (2010). Tumor-conditioned macrophages

secrete migration-stimulating factor: a new marker for M2-polarization, influencing tumor cell motility. Journal of immunology (Baltimore, Md : 1950) *185*, 642-652.

Sotosek, S., Sotosek Tokmadzic, V., Mrakovcic-Sutic, I., Tomas, M.I., Dominovic, M., Tulic, V., Sutic, I., Maricic, A., Sokolic, J., and Sustic, A. (2011). Comparative study of frequency of different lymphocytes subpopulation in peripheral blood of patients with prostate cancer and benign prostatic hyperplasia. Wiener klinische Wochenschrift *123*, 718-725.

Stewart, D.A., Yang, Y., Makowski, L., and Troester, M.A. (2012). Basal-like breast cancer cells induce phenotypic and genomic changes in macrophages. Molecular cancer research : MCR *10*, 727-738.

Szczepanski, M.J., Szajnik, M., Welsh, A., Whiteside, T.L., and Boyiadzis, M. (2011). Blast-derived microvesicles in sera from patients with acute myeloid leukemia suppress natural killer cell function via membrane-associated transforming growth factor-beta1. Haematologica *96*, 1302-1309.

Tahir, S.A., Park, S., and Thompson, T.C. (2009). Caveolin-1 regulates VEGF-stimulated angiogenic activities in prostate cancer and endothelial cells. Cancer Biology & Therapy *8*, 2284-2294.

Tahir, S.A., Yang, G., Ebara, S., Timme, T.L., Satoh, T., Li, L., Goltsov, A., Ittmann, M., Morrisett, J.D., and Thompson, T.C. (2001). Secreted Caveolin-1 Stimulates Cell Survival/Clonal Growth and Contributes to Metastasis in Androgen-insensitive Prostate Cancer. Cancer Research *61*, 3882-3885.

Trudgian, D.C., Ridlova, G., Fischer, R., Mackeen, M.M., Ternette, N., Acuto, O., Kessler, B.M., and Thomas, B. (2011). Comparative evaluation of label-free SINQ normalized spectral index quantitation in the central proteomics facilities pipeline. Proteomics *11*, 2790-2797.

Trudgian, D.C., Thomas, B., McGowan, S.J., Kessler, B.M., Salek, M., and Acuto, O. (2010). CPFP: a central proteomics facilities pipeline. Bioinformatics *26*, 1131-1132.

Utleg, A.G., Yi, E.C., Xie, T., Shannon, P., White, J.T., Goodlett, D.R., Hood, L., and Lin, B. (2003). Proteomic analysis of human prostasomes. The Prostate *56*, 150-161.

Ward, D.M., Vaughn, M.B., Shiflett, S.L., White, P.L., Pollock, A.L., Hill, J., Schnegelberger, R., Sundquist, W.I., and Kaplan, J. (2005). The role of LIP5 and CHMP5 in multivesicular body formation and HIV-1 budding in mammalian cells. The Journal of biological chemistry *280*, 10548-10555.

Wennemuth, G., Aumüller, G., Bacher, M., and Meinhardt, A. (2000). Macrophage Migration Inhibitory Factor-Induced Ca2+ Response in Rat Testicular Peritubular Cells. Biology of Reproduction *62*, 1632-1639.

Wu, K.N., Queenan, M., Brody, J.R., Potoczek, M., Sotgia, F., Lisanti, M.P., and Witkiewicz, A.K. (2011). Loss of stromal caveolin-1 expression in malignant melanoma metastases predicts poor survival. Cell cycle (Georgetown, Tex) *10*, 4250-4255.

Zhang, G., Deinhardt, K., Chao, M.V., and Neubert, T.A. (2011). Study of neurotrophin-3 signaling in primary cultured neurons using multiplex stable isotope labeling with amino acids in cell culture. Journal of proteome research *10*, 2546-2554.